WEST

······································	portrocereconocequire executive conj	Zarrennessen er
Help	Logout	Interrupt

Main Menu | Search Form | Posting Counts | Show's Numbers | Edit's Numbers | Preferences | Cases

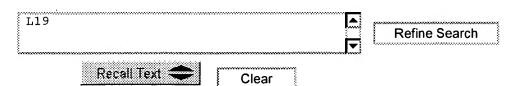
Search Results -

	·
Term	Documents
BEST	930582
BESTS	153
OPTIM\$9	(
OPTIM	119
OPTIMA	2726
OPTIMAAL	2
OPTIMAB	2
OPTIMABILITY	2
OPTIMABLE	2
OPTIMABLY	1
'OPTIMAB.RTM"	5
L17 AND ((OPTIM\$9 OR IDEAL\$5 OR BEST) WITH IMAG\$6))).USPT,PGPB,JPAB,EPAB,DWPI,TDBD.	84

There are more results than shown above. Click here to view the entire set.

	L.
Databass	F
Database:	

Search:



Search History

DATE: Monday, October 27, 2003 Printable Copy Create Case

Set Name		Hit Count	Set Name result set
DB = U	SPT,PGPB,JPAB,EPAB,DWPI,TDBD; PLUR=YES; OP=ADJ		
<u>L19</u>	L17 and ((optim\$9 or ideal\$5 or best) with (imag\$6))	84	<u>L19</u>
<u>L18</u>	L17 and ((optim\$9 or ideal\$5 or best) with (imag46))	0	<u>L18</u>
<u>L17</u>	L16 and (boundar\$6 or artifact\$3 or artefact\$3 or ghost\$5 or blur\$6 or alias\$6 or slab or edg\$4)	97	<u>L17</u>
<u>L16</u>	L14 and ("set" or group\$5 or plurality or sub-set or subset or "subset")	104	<u>L16</u>
<u>L15</u>	L14 and ("set" or group or plurality or sub-set or subset or "sub set")	104	<u>L15</u>
<u>L14</u>	L13 and (kspace or k-space or "k space" or "kx" or "ky" or "kz" or raw or ((image or frequency) with space))	104	<u>L14</u>
<u>L13</u>	L12 and (optim\$9 or ideal\$5 or best)	121	<u>L13</u>
<u>L12</u>	L11 and ((complet\$5 or entir46 or total\$3 or finish\$5 or whole) with (imag\$6))	144	<u>L12</u>
<u>L11</u>	L10 and ((complet\$5 or entir46 or total\$3 or finish\$5 or whole) with ((field of view) or field-of-view or fov))	148	<u>L11</u>
<u>L10</u>	L9 and (complet\$5 or entir46 or total\$3 or finish\$5 or whole)	526	<u>L10</u>
<u>L9</u>	L8 and ((imag\$6) with ((field of view) or field-of-view or fov))	556	<u>L9</u>
<u>L8</u>	L7 and (comput\$6 or proces\$9 or proces\$9 or program\$8)	840	<u>L8</u>
<u>L7</u>	L6 and ((imag\$6) with (scan\$7 or apparatus or device))	840	<u>L7</u>
<u>L6</u>	L5 and (comput\$6 or proces\$9 or proces49 or program\$8)	944	<u>L6</u>
<u>1.5</u>	L4 and (scan\$7 or apparatus or device)	974	<u>L.5</u>
<u>L4</u>	L3 and (direction\$3 or axes or axis or encod\$6 or increment\$5 or step\$8)	1010	<u>L4</u>
<u>L3</u>	L2 and (imag\$6)	1028	<u>L3</u>
<u>L2</u>	L1 and (gradient)	1069	<u>L2</u>
<u>L1</u>	((field of view) or field-of-view or fov)	5084	<u>L1</u>

END OF SEARCH HISTORY

WEST

Generate Collection

Print

Search Results - Record(s) 1 through 84 of 84 returned.

1. Document ID: US 20030189098 A1

L19: Entry 1 of 84

File: PGPB

Oct 9, 2003

PGPUB-DOCUMENT-NUMBER: 20030189098

PGPUB-FILING-TYPE: new

DOCUMENT-IDENTIFIER: US 20030189098 A1

TITLE: Planar light illumination and $\underline{imaging}$ (PLIIM) systems employing LED-based planar light illumination arrays (PLIAS) and linear electronic \underline{image} detection

arrays

PUBLICATION-DATE: October 9, 2003

INVENTOR-INFORMATION:

NAME	CITY	STATE	COUNTRY	RULE-47
Tsikos, Constantine J.	Voorhees	NJ	US	
Good, Timothy A.	Clementon	NJ	US	
Schnee, Michael D.	Aston	PA	US	
Zhu, Xiaoxun	Marlton	NJ	US	
Amundsen, Thomas	Turnersville	NJ	US	
Knowles, C. Harry	Moorestown	NJ	US	

US-CL-CURRENT: 235/454

Full Title Citation Front Review Classification Date Reference Sequences Attachments Claims KMC	
### ### ### ### ### #### #### ########	
Draw Desc Image	

2. Document ID: US 20030150917 A1

L19: Entry 2 of 84

File: PGPB

Aug 14, 2003

PGPUB-DOCUMENT-NUMBER: 20030150917

PGPUB-FILING-TYPE: new

DOCUMENT-IDENTIFIER: US 20030150917 A1

TITLE: Planar light illumination and $\underline{imaging}$ (PLIIM) system employing led-based planar light illumination arrays (PLIAS) and an area-type \underline{image} detection array

PUBLICATION-DATE: August 14, 2003

NAME CITY STATE COUNTRY RULE-47 Voorhees NJ US Tsikos, Constantine J. Clementon US N.T Good, Timothy Schnee, Michael D. Aston PA US US NJ Zhu, Xiaoxun Marlton Amundsen, Thomas Turnersville NJ US US Knowles, C. Harry Moorestown NJ

US-CL-CURRENT: 235/454

Full Title Citation Front Review Classification Date Reference Sequences Attachments Claims EMIC Draw Desc Image

3. Document ID: US 20030150916 A1

L19: Entry 3 of 84

File: PGPB

Aug 14, 2003

PGPUB-DOCUMENT-NUMBER: 20030150916

PGPUB-FILING-TYPE: new

DOCUMENT-IDENTIFIER: US 20030150916 A1

TITLE: LED-based planar light illumination and imaging (PLIIM) systems

PUBLICATION-DATE: August 14, 2003

INVENTOR-INFORMATION:

COUNTRY RULE-47 NAME CITY STATE US Tsikos, Constantine J. Voorhees NJ Clementon NJ US Good, Timothy Aston PΑ US Schnee, Michael D. NJ US Zhu, Xiaoxun Marlton Amundsen, Thomas Turnersville NJ US US Knowles, C. Harry Moorestown ŊJ

US-CL-CURRENT: 235/454

Full Title Citation Front Review Classification Date Reference Sequences Attachments 1990 |
Draw Desc | Image |

4. Document ID: US 20030146282 A1

L19: Entry 4 of 84

File: PGPB

Aug 7, 2003

PGPUB-DOCUMENT-NUMBER: 20030146282

PGPUB-FILING-TYPE: new

DOCUMENT-IDENTIFIER: US 20030146282 A1

TITLE: Bioptical product and produce identification systems employing planar laser

illumination and imaging (PLIM) based subsystems

PUBLICATION-DATE: August 7, 2003

NAME	CITY	STATE	COUNTRY	RULE-47
Tsikos, Constantine J.	Voorhees	NJ	US	
Wirth, Allan	Bedford	MA	US	
Good, Timothy A.	Clementon	NJ	US	
Jankevics, Andrew	Westford	MA	US	
Kim, Steve Y.	Cambridge	MA	US	
Amundsen, Thomas	Turnersville	NJ	US	
Naylor, Charles A.	Sewell	NJ	US	
Dobbs, Russell Joseph	Cherry Hill	NJ	US	
Giordano, Patrick A.	Blackwood	NJ	US	
Yorsz, Jeffery	Winchester	MA	US	
Schmidt, Mark S.	Williamstown	NJ	US	
Colavito, Stephen J.	Brookhaven	PA	US	
Wilz, David M. SR.	Sewell	NJ	US	
Au, Ka Man	Philadelphia	PA	US	
Svedas, William	Deptford	NJ	US	
Ghosh, Sankar	Glenolden	PA	US	
Schnee, Michael D.	Aston	PA	US	
Zhu, Xiaoxun	Marlton	NJ	US	
Knowles, C. Harry	Moorestown	NJ	US	

US-CL-CURRENT: 235/454

Full Title Citation	Front Review Clas	emication Date R	eference Sequences	Attachments	KUMC
Draw Deso Image					
	•				

5. Document ID: US 20030135111 A1

L19: Entry 5 of 84

File: PGPB

Jul 17, 2003

PGPUB-DOCUMENT-NUMBER: 20030135111

PGPUB-FILING-TYPE: new

DOCUMENT-IDENTIFIER: US 20030135111 A1

TITLE: Method and apparatus for magnetic resonance arteriography using contrast

agents

PUBLICATION-DATE: July 17, 2003

INVENTOR-INFORMATION:

NAME

CITY

STATE

RULE-47

Meaney, James F.M.

Leeds

ΜI

GB

COUNTRY

Prince, Martin R.

Ann Arbor

US

US-CL-CURRENT: 600/422

Full Title Citation Front Review Classification Date Reference Sequences Attachments	1000C
Draw Desc Image	

6. Document ID: US 20030114748 A1

L19: Entry 6 of 84

File: PGPB

Jun 19, 2003

PGPUB-DOCUMENT-NUMBER: 20030114748

PGPUB-FILING-TYPE: new

DOCUMENT-IDENTIFIER: US 20030114748 A1

TITLE: Inherently de-coupled sandwiched solenoidal array coil

PUBLICATION-DATE: June 19, 2003

INVENTOR-INFORMATION:

NAME CITY STATE COUNTRY RULE-47

South San Francisco CA US Su, Sunyu San Francisco CA US Kaufman, Leon Arakawa, Mitsuaki CA US Hillsborough Carlson, Joseph W. Kensington CA US

US-CL-CURRENT: 600/422

Full | Title | Citation | Front | Review | Classification | Date | Reference | Sequences | Attachments |
Draw Desc | Image |

7. Document ID: US 20030109782 A1

L19: Entry 7 of 84 File: PGPB Jun 12, 2003

PGPUB-DOCUMENT-NUMBER: 20030109782

PGPUB-FILING-TYPE: new

DOCUMENT-IDENTIFIER: US 20030109782 A1

TITLE: Inherently de-coupled sandwiched solenoidal array coil

PUBLICATION-DATE: June 12, 2003

INVENTOR-INFORMATION:

NAME CITY STATE COUNTRY RULE-47

Su, Sunyu South San Francisco CA US Kaufman, Leon San Francisco CA US

US-CL-CURRENT: 600/421

Full Title Citation Front Review Classification Date Reference Sequences Attachments KNAC |
Draw Desc Image

8. Document ID: US 20030102379 A1

L19: Entry 8 of 84 File: PGPB Jun 5, 2003

PGPUB-DOCUMENT-NUMBER: 20030102379

PGPUB-FILING-TYPE: new

DOCUMENT-IDENTIFIER: US 20030102379 A1

TITLE: LED-based planar light illumination and imaging (PLIIM) engine

PUBLICATION-DATE: June 5, 2003

Kinc

INVENTOR-INFORMATION:

NAME CITY STATE COUNTRY RULE-47 Tsikos, Constantine J. Voorhees NJ US Knowles, C. Harry Moorestown NJ US Good, Timothy A. Clementon US NJ Schnee, Michael D. Aston PA US Zhu, Xiaoxun Marlton ŊJ US Amundsen, Thomas Turnersville US NJ Schmidt, Mark C. Williamstown NJ US Giordano, Patrick A. Blackwood NJ US

US-CL-CURRENT: 235/462.45

Full Title Citation Front Review Classification Date Reference Sequences Attachments Draw Desc Image KWC

9. Document ID: US 20030100825 A1

L19: Entry 9 of 84

File: PGPB

May 29, 2003

PGPUB-DOCUMENT-NUMBER: 20030100825

PGPUB-FILING-TYPE: new

DOCUMENT-IDENTIFIER: US 20030100825 A1

TITLE: METHOD AND SYSTEM FOR EXTENDED VOLUME IMAGING USING MRI

PUBLICATION-DATE: May 29, 2003

INVENTOR-INFORMATION:

NAME CITY STATE COUNTRY RULE-47

Demoulin, Charles Lucian Ballston Lake NY US
Zhu, Yudong Clifton Park NY US

US-CL-CURRENT: 600/410

Full Title Citation Front Review Classification Date Reference Sequences Attachments.

Draw Desc Image

Kilde

10. Document ID: US 20030098353 A1

L19: Entry 10 of 84

File: PGPB

May 29, 2003

PGPUB-DOCUMENT-NUMBER: 20030098353

PGPUB-FILING-TYPE: new

DOCUMENT-IDENTIFIER: US 20030098353 A1

TITLE: Planar laser illumination and imaging (PLIIM) engine

PUBLICATION-DATE: May 29, 2003

Tsikos, Constantine J. Voorhees NJ US
Tairda, comacanerne a. Voorneed
Knowles, C. Harry Moorestown NJ US
Zhu, Xiaoxun Marlton NJ US
Schnee, Michael D. Aston PA US
Amundsen, Thomas Turnersville NJ US
Schmidt, Mark C. Williamstown NJ US
Giordano, Patrick A. Blackwood NJ US

US-CL-CURRENT: <u>235/472.01</u>

Full Title Citation Front Review Classification Date Reference Sequences Attachments NMC Praw Desc Image

11. Document ID: US 20030098349 A1

L19: Entry 11 of 84

File: PGPB

May 29, 2003

PGPUB-DOCUMENT-NUMBER: 20030098349

PGPUB-FILING-TYPE: new

DOCUMENT-IDENTIFIER: US 20030098349 A1

TITLE: Hand-supportable planar laser illumination and $\frac{\text{imaging}}{\text{optically-combined planar}}$ employing linear electronic $\frac{\text{image}}{\text{image}}$ detection arrays and $\frac{\text{optically-combined planar}}{\text{optically-combined planar}}$ laser illumination beams (PLIBS) produced from a multiplicity of laser diode sources to achieve a reduction in speckle-pattern noise power in said PLIIM $\frac{\text{devices}}{\text{devices}}$

PUBLICATION-DATE: May 29, 2003

INVENTOR-INFORMATION:

NAME CITY STATE COUNTRY RULE-47 Tsikos, Constantine J. Voorhees NJ US Knowles, C. Harry Moorestown NJ US Zhu, Xiaoxun Marlton NJ US Schnee, Michael D. Aston PΑ US US Good, Timothy A. Clementon NJ

US-CL-CURRENT: 235/462.01

Full Title Citation Front Review Classification Date Reference Sequences Attachments KMC Draw Desc. Image

12. Document ID: US 20030094495 A1

L19: Entry 12 of 84

File: PGPB

May 22, 2003

PGPUB-DOCUMENT-NUMBER: 20030094495

PGPUB-FILING-TYPE: new

DOCUMENT-IDENTIFIER: US 20030094495 A1

 $\begin{array}{ll} \hbox{\tt TITLE: Nuclear resonance based} & \underline{\text{\tt scanning}} & \hbox{\tt system having an automatic object} \\ \hbox{\tt identification and attribute information acquisition and linking mechanism} \end{array}$

integrated therein

PUBLICATION-DATE: May 22, 2003

INVENTOR-INFORMATION:

NAME CITY STATE COUNTRY RULE-47

Knowles, C. Harry Moorestown NJ US Schmidt, Mark C. Williamstown NJ US Fisher, Dale Voorhees NJ US

US-CL-CURRENT: 235/462.14

13. Document ID: US 20030089778 A1

L19: Entry 13 of 84 File: PGPB May 15, 2003

PGPUB-DOCUMENT-NUMBER: 20030089778

PGPUB-FILING-TYPE: new

DOCUMENT-IDENTIFIER: US 20030089778 A1

TITLE: Method of and system for automatically producing digital <u>images</u> of a moving object, with pixels having a substantially uniform white level independent of the velocity of said moving object

PUBLICATION-DATE: May 15, 2003

INVENTOR-INFORMATION:

NAME CITY STATE COUNTRY RULE-47 Tsikos, Constantine J. NJ US Voorhees US Knowles, C. Harry Moorestown NJ US Zhu, Xiaoxun Marlton NJ Schnee, Michael D. Aston PΑ US Au, Ka Man Philadelphia PA US Wirth, Allan Bedford MA US Good, Timothy A. Clementon ŊJ US Ghosh, Sankar Glenolden PA US Turnersville US Amundsen, Thomas N.T

US-CL-CURRENT: 235/454

Full | Title | Citation | Front | Review | Classification | Date | Reference | Sequences | Attachments | KMC | Draw Desc | Image |

14. Document ID: US 20030085281 A1

L19: Entry 14 of 84 File: PGPB May 8, 2003

PGPUB-DOCUMENT-NUMBER: 20030085281

PGPUB-FILING-TYPE: new

DOCUMENT-IDENTIFIER: US 20030085281 A1

TITLE: Tunnel-type package identification system having a remote station with an ethernet-over-fiber-optic data communication link

7 of 45 10/27/2003 9:15 AM

COUNTRY

US

US

PUBLICATION-DATE: May 8, 2003

INVENTOR-INFORMATION:

NAME

CITY

STATE

RULE-47

Knowles, C. Harry

Kim, Steven Y.

Moorestown

NJ

Cambridge MA

US-CL-CURRENT: 235/454

Full | Title | Citation | Front | Review | Classification | Date | Reference | Sequences | Attachments | Draw Desc | Image |

15. Document ID: US 20030085280 A1

L19: Entry 15 of 84

File: PGPB

May 8, 2003

KUME

PGPUB-DOCUMENT-NUMBER: 20030085280

PGPUB-FILING-TYPE: new

DOCUMENT-IDENTIFIER: US 20030085280 A1

TITLE: Method of speckle-noise pattern reduction and <u>apparatus</u> therefor based on reducing the spatial-coherence of the planar laser illumination beam before it illuminates the target object by applying spatial intensity modulation techniques during the transmission of the PLIB towards the target

PUBLICATION-DATE: May 8, 2003

INVENTOR-INFORMATION:

NAME CITY STATE COUNTRY RULE-47 Tsikos, Constantine J. Voorhees ŊJ US Knowles, C. Harry Moorestown NJ US Wirth, Allan Bedford MA US Clementon NJ US Good, Timothy A. Westford MA US Jankevics, Andrew

US-CL-CURRENT: 235/454

Full Title Citation Front Review Classification Date Reference Sequences Attachments Draw Desc Image

KWAC

16. Document ID: US 20030080192 A1

L19: Entry 16 of 84

File: PGPB

May 1, 2003

PGPUB-DOCUMENT-NUMBER: 20030080192

PGPUB-FILING-TYPE: new

DOCUMENT-IDENTIFIER: US 20030080192 A1

TITLE: Neutron-beam based scanning system having an automatic object identification

and attribute information acquisition and linking mechanism integrated therein

PUBLICATION-DATE: May 1, 2003

NAME	CITY	STATE	COUNTRY	RULE-47
Tsikos, Constantine J.	Voorhees	NJ	US	
Knowles, C. Harry	Moorestown	ИJ	US	
Zhu, Xiaoxun	Marlton	NJ	US	
Schnee, Michael D.	Aston	PA	US	
Au, Ka Man	Philadelphia	PA	US	
Wirth, Allan	Bedford	MA	US	
Good, Timothy A.	Clementon	NJ	US	
Jankevics, Andrew	Westford	MA	US	
Ghosh, Sankar	Glenolden	PA	US	
Naylor, Charles A.	Sewell	NJ	US	
Amundsen, Thomas	Turnersville	NJ	US	
Blake, Robert	Woodbury Heights	NJ	US	
Svedas, William	Deptford	NJ	US	
Defoney, Shawn	Runnemede	NJ	US	
Skypala, Edward	Blackwood	NJ	US	
Vatan, Pirooz	Wilmington	MA	US	
Dobbs, Russell Joseph	Cherry Hill	NJ	US	
Kolis, George	Pennsauken	NJ	US	
Schmidt, Mark C.	Williamstown	NJ	US	
Yorsz, Jeffery	Winchester	MA	US	
Giordano, Patrick A.	Blackwood	NJ	US	
Colavito, Stephen J.	Brookhaven	PA	US	
Wilz, David W. SR.	Sewell	NJ	US	
Schwartz, Barry E.	Haddonfield	NJ	US	
Kim, Steven Y.	Cambridge	MA	US	
Fisher, Dale	Voorhees	NJ	US	
Tassell, Jon Van	Winchester	MA	US	

US-CL-CURRENT: 235/462.14

Full Title Citation Front Review Classification Date Reference Sequences Attachments	Kulac
Draw base Image	

17. Document ID: US 20030080190 A1

L19: Entry 17 of 84 File: PGPB May 1, 2003

PGPUB-DOCUMENT-NUMBER: 20030080190

PGPUB-FILING-TYPE: new

DOCUMENT-IDENTIFIER: US 20030080190 A1

TITLE: Method of and system for automatically producing digital $\frac{images}{object}$, with pixels having a substantially uniform white level independent of the velocity of said moving object

PUBLICATION-DATE: May 1, 2003

INVENTOR-INFORMATION:

9 of 45 10/27/2003 9:15 AM

NAME	CITY	STATE	COUNTRY	RULE-47
Tsikos, Constantine J.	Voorhees	NJ	US	
Knowles, C. Harry	Moorestown	NJ	US	
Zhu, Xiaoxun	Marlton	NJ	US	
Schnee, Michael D.	Aston	PA	US	
Au, Ka Man	Philadelphia	PA	US	
Wirth, Allan	Bedford	MA	US	
Good, Timothy A.	Clementon	NJ	US	
Jankevics, Andrew	Westford	MA	US	
Ghosh, Sankar	Glenolden	PA	US	
Naylor, Charles A.	Sewell	NJ	US	
Amundsen, Thomas	Turnersville	NJ	US	
Blake, Robert	Woodbury Heights	NJ	US	
Svedas, William	Deptford	NJ	US	
Defoney, Shawn	Runnemede	NJ	US	
Skypala, Edward	Blackwood	NJ	US .	
Vatan, Pirooz	Wilmington	MA	US	
Dobbs, Russell Joseph	Cherry Hill	NJ	US	
Kolis, George	Pennsauken	NJ	US	
Schmidt, Mark C.	Williamstown	NJ	US	
Yorsz, Jeffery	Winchester	MA	US	
Giordano, Patrick A.	Blackwood	NJ	US	
Colavito, <u>Stephen</u> J.	Brookhaven	PA	US	
Wilz, David W. SR.	Sewell	NJ	US	
Schwartz, Barry E.	Haddonfield	NJ	US	
Kim, Steven Y.	Cambridge	MA	US	
Fisher, Dale	Voorhees	NJ	US	
Tassell, Jon Van	Winchester	MA	US	

US-CL-CURRENT: 235/462.01

Full Title Citation Front Review Classification Date Reference Sequences	Attachments KMC
Braw Desc Amage	

18. Document ID: US 20030071128 A1

L19: Entry 18 of 84

File: PGPB

Apr 17, 2003

PGPUB-DOCUMENT-NUMBER: 20030071128

PGPUB-FILING-TYPE: new

DOCUMENT-IDENTIFIER: US 20030071128 A1

TITLE: Led-based planar light illumination and $\frac{imaging}{and}$ (PLIIM) based camera system employing real-time object coordinate acquistion and producing to control automatic zoom and focus $\frac{imaging}{and}$ optics

PUBLICATION-DATE: April 17, 2003

Apr 17, 2003

NAME	CITY	STATE	COUNTRY	RULE-47
Tsikos, Constantine J.	Voorhees	NJ	US	
Knowles, C. Harry	Moorestown	NJ	US	
Zhu, Xiaoxun	Marlton	NJ	US	
Schnee, Michael D.	Aston	PA	US	
Au, Ka Man	Philadelphia	PA	US	
Good, Timothy A.	Clementon	NJ	US	
Ghosh, Sankar	Glenolden	PA	US	
Amundsen, Thomas	Turnersville	NJ	US	

Full Title Citation Front Review Classification Date Reference Sequences Attentments

US-CL-CURRENT: 235/470

	881 884446881
Rraw Pesc Image	

File: PGPB

19. Document ID: US 20030071124 A1

PGPUB-DOCUMENT-NUMBER: 20030071124 PGPUB-FILING-TYPE: new

L19: Entry 19 of 84

DOCUMENT-IDENTIFIER: US 20030071124 A1

TITLE: Method of speckle-noise pattern reduction and <u>apparatus</u> therefor based on reducing the temporal-coherence of the planar laser illumination beam before it illuminates the target object by applying temporal phase modulation techniques during the transmission of the PLIB towards the target

PUBLICATION-DATE: April 17, 2003

NAME	CITY	STATE	COUNTRY	RULE-47
Tsikos, Constantine J.	Voorhees	NJ	US	
Knowles, C. Harry	Moorestown	NJ	US	
Zhu, Xiaoxun	Marlton	NJ	US	
Schnee, Michael D.	Aston	PA	US	
Au, Ka Man	Philadelphia	PA	US	
Wirth, Allan	Bedford	MA	US	
Good, Timothy A.	Clementon	NJ	US	
Jankevics, Andrew	Westford	MA	US	
Ghosh, Sankar	Glenolden	PA	US	
Naylor, Charles A.	Sewell	NJ	US	
Amundsen, Thomas	Turnersville	NJ	US	
Blake, Robert	Woodbury Heights	NJ	US	
Svedas, William	Deptford	NJ	US	
Defoney, Shawn	Runnemede	NJ	US	
Skypala, Edward	Blackwood	NJ	US	
Vatan, Pirooz	Wilmington	MA	US	
Dobbs, Russell Joseph	Cherry Hill	NJ	US	
Kolis, George	Pennsauken	NJ	US	
Schmidt, Mark C.	Williamstown	NJ	US	
Yorsz, Jeffery	Winchester	MA	US	
Giordano, Patrick A.	Blackwood	NJ	US	
Colavito, Stephen J.	Brookhaven	PA	US	
Wilz, David W. SR.	Sewell	NJ	US	
Schwartz, Barry E.	Haddonfield	NJ	US	
Kim, Steven Y.	Cambridge	MA	US	
Fisher, Dale	Voorhees	NJ	US	
Tassell, Jon Van	Winchester	MA	US	

US-CL-CURRENT: 235/454

Full Title Citation Front Review Classification Date Reference Sequences Attachments Killion

x

20. Document ID: US 20030071123 A1

L19: Entry 20 of 84

File: PGPB

Apr 17, 2003

PGPUB-DOCUMENT-NUMBER: 20030071123

PGPUB-FILING-TYPE: new

DOCUMENT-IDENTIFIER: US 20030071123 A1

TITLE: Method of speckle-noise pattern reduction and <u>apparatus</u> therefor based on reducing the temporal coherence of the planar laser illumination beam before it illuminates the target object by applying temporal intensity modulation techniques during the transmission of the PLIB towards the target

PUBLICATION-DATE: April 17, 2003

NAME CITY STATE COUNTRY RULE-47 Tsikos, Constantine J. Voorhees N.T HS Knowles, C. Harry US Moorestown NJWirth, Allan Bedford MA US Good, Timothy A. Clementon NJ US Jankevics, Andrew Westford MA US

US-CL-CURRENT: 235/454

Full Title Citation Front Review Classification Date Reference Sequences Affachments

Draw Desc Image

KOMC

21. Document ID: US 20030071122 A1

L19: Entry 21 of 84

File: PGPB

Apr 17, 2003

PGPUB-DOCUMENT-NUMBER: 20030071122

PGPUB-FILING-TYPE: new

DOCUMENT-IDENTIFIER: US 20030071122 A1

TITLE: Internet-based method of and system for remotely monitoring, configuring and servicing planar laser illumination and imaging (PLIIM) based networks with nodes for supporting object identification and attribute information acquisition functions

PUBLICATION-DATE: April 17, 2003

INVENTOR-INFORMATION:

NAME CITY STATE COUNTRY RULE-47 Tsikos, Constantine J. Voorhees ŊJ US Knowles, C. Harry US Moorestown NJUS Zhu, Xiaoxun Marlton NJ US Au, Ka Man Philadelphia PΑ Schwartz, Barry E. Haddonfield NJ US

US-CL-CURRENT: 235/454

Full Title Citation Front Review Classification Date Reference Sequences Attachments Draw Desc Image

22. Document ID: US 20030071119 A1

L19: Entry 22 of 84

File: PGPB

Apr 17, 2003

PGPUB-DOCUMENT-NUMBER: 20030071119

PGPUB-FILING-TYPE: new

DOCUMENT-IDENTIFIER: US 20030071119 A1

TITLE: Method of and apparatus for automatically compensating for viewing-angle distortion in digital linear \underline{images} of object surfaces moving past a planar laser illumination and $\underline{imaging}$ (PLIIM) based camera system at skewed viewing angles

PUBLICATION-DATE: April 17, 2003

NAME CITY STATE COUNTRY RULE-47 Tsikos, Constantine J. Voorhees NJ US Knowles, C. Harry Moorestown US NJZhu, Xiaoxun Marlton NJ US Schnee, Michael D. US Aston PA Philadelphia PA US Au, Ka Man Ghosh, Sankar Glenolden PA US

US-CL-CURRENT: 235/434

Full Title Citation Front Review Classification Date Reference Sequences Attachments	PARME
Draw Desc. Image	
	•••••••••••••••••••••••••••••••••••••••

23. Document ID: US 20030062415 A1

L19: Entry 23 of 84

File: PGPB

Apr 3, 2003

PGPUB-DOCUMENT-NUMBER: 20030062415

PGPUB-FILING-TYPE: new

DOCUMENT-IDENTIFIER: US 20030062415 A1

TITLE: Planar laser illumination and $\frac{imaging}{image}$ (PLIIM) based camera system for automatically producing digital linear $\frac{images}{image}$ of a moving object, containing pixels having a substantially square aspectratio independent of the measured range and/or velocity of said moving object

PUBLICATION-DATE: April 3, 2003

INVENTOR-INFORMATION:

NAME	CITY	STATE	COUNTRY	RULE-47
Tsikos, Constantine J.	Voorhees	NJ	US	
Knowles, C. Harry	Moorestown	NJ	US	
Zhu, Xiaoxun	Marlton	NJ	US	
Schnee, Michael D.	Aston	PA	US	
Au, Ka Man	Philadelphia	PA	US	
Wirth, Allan	Bedford	MA	US	
Ghosh, Sankar	Glenolden	PA	US	

US-CL-CURRENT: 235/454

Drabit	Title	: Citation Front Review Classification Date Reference Sequences Attachin Image	vents KuMC
	24.	Document ID: US 20030062414 A1	

File: PGPB

PGPUB-DOCUMENT-NUMBER: 20030062414

PGPUB-FILING-TYPE: new

L19: Entry 24 of 84

DOCUMENT-IDENTIFIER: US 20030062414 A1

TITLE: Method of and apparatus for automatically cropping captured linear images of a moving object prior to image processing using region of interest (ROI) coordinate

Apr 3, 2003

specifications captured by an object profiling subsystem

PUBLICATION-DATE: April 3, 2003

INVENTOR - INFORMATION:

CITY STATE COUNTRY RULE-47 NAME

Tsikos, Constantine J. Voorhees NJ US Knowles, C. Harry US Moorestown NJ Zhu, Xiaoxun Marlton NJ US Au, Ka Man Philadelphia PΑ US

Ghosh, Sankar Glenolden PΑ US

US-CL-CURRENT: 235/454

Full Title Citation Front Review Classification Date Reference Sequences Attachments Drawit Desc Image

Killic

25. Document ID: US 20030060698 A1

L19: Entry 25 of 84 File: PGPB Mar 27, 2003

PGPUB-DOCUMENT-NUMBER: 20030060698

PGPUB-FILING-TYPE: new

DOCUMENT-IDENTIFIER: US 20030060698 A1

TITLE: Magnetic resonance angiography using floating table projection imaging

PUBLICATION-DATE: March 27, 2003

INVENTOR-INFORMATION:

CITY STATE COUNTRY RULE-47 NAME

Madison WI US Mistretta, Charles A.

US-CL-CURRENT: 600/410

Title Citation Front Review Classification Date Reference Sequences Attachments Draw Desc Image

KOME

26. Document ID: US 20030055330 A1

L19: Entry 26 of 84 File: PGPB Mar 20, 2003

PGPUB-DOCUMENT-NUMBER: 20030055330

PGPUB-FILING-TYPE: new

DOCUMENT-IDENTIFIER: US 20030055330 A1

TITLE: Sensitivity encoding MRI acquisition method

PUBLICATION-DATE: March 20, 2003

INVENTOR-INFORMATION:

COUNTRY NAME CITY STATE RULE-47

King, Kevin F. New Berlin WΙ US Angelos, Lisa C. Hartland ΝI US

US-CL-CURRENT: 600/410; 702/28

Full Title Citation Front Review Classification Date Reference Sequences Attachments

Draw Desp. Image

Kunc

27. Document ID: US 20030053513 A1

L19: Entry 27 of 84

File: PGPB

Mar 20, 2003

PGPUB-DOCUMENT-NUMBER: 20030053513

PGPUB-FILING-TYPE: new

DOCUMENT-IDENTIFIER: US 20030053513 A1

TITLE: Method of and system for producing high-resolution 3-D images of 3-D object

surfaces having arbitrary surface geometry

PUBLICATION-DATE: March 20, 2003

INVENTOR-INFORMATION:

CITY STATE COUNTRY RULE-47 NAME Vatan, Pirooz Lexington MA US Knowles, C. Harry Moorestown NJ US Marlton NJ US Zhu, Xiaoxun Tsikos, Constantine J. Voorhees NJ US

US-CL-CURRENT: 372/109; 385/93

Full | Title | Citation | Front | Review | Classification | Date | Reference | Sequences | Attachments | Drain Desc | Image |

KNWE

28. Document ID: US 20030052175 A1

L19: Entry 28 of 84

File: PGPB

Mar 20, 2003

PGPUB-DOCUMENT-NUMBER: 20030052175

PGPUB-FILING-TYPE: new

DOCUMENT-IDENTIFIER: US 20030052175 A1

TITLE: Method of and system for automatically producing digital \underline{images} of moving objects, with pixels having a substantially uniform white level independent of the

velocities of the moving objects

PUBLICATION-DATE: March 20, 2003

|--|--|--|

NAME	CITY	STATE	COUNTRY	RULE-47
Tsikos, Constantine J.	Voorhees	NJ	US	
Knowles, C. Harry	Moorestown	NJ	US	
Zhu, Xiaoxun	Marlton	NJ	US	
Schnee, Michael D.	Aston	PA	US	
Au, Ka Man	Philadelphia	PA	US	
Wirth, Allan	Bedford	MA	US	
Good, Timothy A.	Clementon	NJ	US	
Jankevics, Andrew	Westford	MA	US	
Ghosh, Sankar	Glenolden	PA	US	
Naylor, Charles A.	Sewell	NJ	US	
Amundsen, Thomas	Turnersville	NJ	US	
Blake, Robert	Woodbury Heights	NJ	US	
Svedas, William	Deptford	NJ	US	
Defoney, Shawn	Runnemede	NJ	US	
Skypala, Edward	Blackwood	NJ	US	
Vatan, Pirooz	Wilmington	MA	US	
Dobbs, Russell Joseph	Cherry Hill	NJ	US	
Kolis, George	Pennsauken	NJ	US	
Schmidt, Mark C.	Williamstown	NJ	US	
Yorsz, Jeffery	Winchester	MA	US	
Giordano, Patrick A.	Blackwood	NJ	US	
Colavito, <u>Stephen</u> J.	Brookhaven	PA	US	
Wilz, David W. SR.	Sewell	NJ	US	
Schwartz, Barry E.	Haddonfield	NJ	US	
Kim, Steven Y.	Cambridge	MA	US	
Fisher, Dale	Voorhees	NJ	US	
Van Tassell, Jon	Winchester	MA	US	

US-CL-CURRENT: 235/472.01

Full | Title | Citation | Front | Review | Classification | Date | Reference | Sequences | Attachments | KWAC |
Draw Desc | Image |

×-----

29. Document ID: US 20030052169 A1

L19: Entry 29 of 84

File: PGPB

Mar 20, 2003

PGPUB-DOCUMENT-NUMBER: 20030052169

PGPUB-FILING-TYPE: new

DOCUMENT-IDENTIFIER: US 20030052169 A1

TITLE: Planar laser illumination and imaging (PLIIM) based camera system for

producing high-resolution 3-D <u>images</u> of moving 3-D objects

PUBLICATION-DATE: March 20, 2003



NAME Tsikos, Constantine J. Knowles, C. Harry Zhu, Xiaoxun Vatan, Pirooz CITY STATE COUNTRY
Voorhees NJ US
Moorestown NJ US
Marlton NJ US
Wilmington MA US

US-CL-CURRENT: 235/454

Full Title Citation Front Review Classification Date Reference Sequences Attachments Draw Desc Image KWAC

RULE-47

30. Document ID: US 20030047597 A1

L19: Entry 30 of 84

File: PGPB

Mar 13, 2003

PGPUB-DOCUMENT-NUMBER: 20030047597

PGPUB-FILING-TYPE: new

DOCUMENT-IDENTIFIER: US 20030047597 A1

TITLE: Programmable data element queuing, handling, processing and linking device integrated into an object identification and attribute acquisition system

PUBLICATION-DATE: March 13, 2003

INVENTOR-INFORMATION:

NAME CITY STATE COUNTRY RULE-47 Knowles, C. Harry Moorestown N.T US US Defoney, Shawn Runnemede NJ Skypala, Edward Blackwood NJ US Schmidt, Mark C. Williamstown NJ US

US-CL-CURRENT: 235/375

Full Title Citation Front Review Classification Date Reference Sequences Attachments Draw Desc Image

KWAC

31. Document ID: US 20030042315 A1

L19: Entry 31 of 84

File: PGPB

Mar 6, 2003

PGPUB-DOCUMENT-NUMBER: 20030042315

PGPUB-FILING-TYPE: new

DOCUMENT-IDENTIFIER: US 20030042315 A1

TITLE: Hand-supportable planar laser illumination and $\underline{imaging}$ (PLIIM) based camera system capable of producing digital linear \underline{images} of a object, containing pixels having a substantially uniform white level independent of the velocity of the object while manually moving said PLIIM based camera system past said object during illumination and $\underline{imaging}$ operations

x

PUBLICATION-DATE: March 6, 2003

Mar 6, 2003



NAME	CITY	STATE	COUNTRY	RULE-47
Tsikos, Constantine J.	Voorhees	NJ	US	
Knowles, C. Harry	Moorestown	NJ	US	
Zhu, Xiaoxun	Marlton	NJ	US	
Schnee, Michael D.	Aston	PA	US	
Au, Ka Man	Philadelphia	PA	US	
Ghosh, Sankar	Glenolden	PA	US	

US-CL-CURRENT: 235/472.01

Full Draw	Title Desc	Citation Front Image	Review Classification Date Reference Sequences Attachments	EMAC
	32.		US 20030042314 A1	

File: PGPB

PGPUB-DOCUMENT-NUMBER: 20030042314

PGPUB-FILING-TYPE: new

L19: Entry 32 of 84

DOCUMENT-IDENTIFIER: US 20030042314 A1

TITLE: Hand-supportable planar laser illumination and $\underline{imaging}$ (PLIIM) \underline{device} employing a pair of linear laser diode arrays mounted about an area \underline{image} detection array, for illuminating an object to be \underline{imaged} with a plurality of optically-combined spatially-incoherent planar laser illumination beams (PLIBS) $\underline{scanned}$ through the field of view (\underline{FOV}) of said area \underline{image} detection array, and reducing the speckle-pattern noise power in detected 2-D \underline{images} by temporally-averaging detected speckle-noise patterns during the photo-integration time period of said area \underline{image} detection array

PUBLICATION-DATE: March 6, 2003

INVENTOR-INFORMATION:

NAME	CITY	STATE	COUNTRY	RULE-47
Tsikos, Constantine J.	Voorhees	NJ	US	
Knowles, C. Harry	Moorestown	NJ	US	
Zhu, Xiaoxun	Marlton	NJ	US	
Schnee, Michael D.	Aston	PA	US	
Wirth, Allan	Bedford	MA	US	
Good, Timothy A.	Clementon	NJ	US	

US-CL-CURRENT: 235/472.01

Full	Title	Citation Front Review Classification Date Reference Sequences Attachments KMC
Draw	Desc	lmage i
*************	*********	
	33.	Document ID: US 20030042309 A1

File: PGPB

PGPUB-DOCUMENT-NUMBER: 20030042309

PGPUB-FILING-TYPE: new

L19: Entry 33 of 84

DOCUMENT-IDENTIFIER: US 20030042309 A1

19 of 45

Mar 6, 2003

TITLE: Generalized method of speckle-noise pattern reduction and particular forms of apparatus therefor based on reducing the spatial-coherence of the planar laser illumination beam after it illuminates the target by applying spatial intensity modulation techniques during the detection of the reflected/scattered PLIB

PUBLICATION-DATE: March 6, 2003

INVENTOR-INFORMATION:

CITY	STATE	COUNTRY	RULE-47
Voorhees	NJ	US	
Moorestown	NJ	US	
Bedford	MA	US	
Westford	MA	US	
Clementon	NJ	US	
	Voorhees Moorestown Bedford Westford	Voorhees NJ Moorestown NJ Bedford MA Westford MA	Voorhees NJ US Moorestown NJ US Bedford MA US Westford MA US

US-CL-CURRENT: 235/454

	Front Review Classification	Flate Reference Semience	es Atiacamenia
**************************************	MARKATAN MAR	CONTRACTOR DESCRIPTION OF THE PROPERTY OF THE	2226 2846 1127 224 114 124 125 125 125 125 125 125 125 125 125 125
Draw Desc Image			

File: PGPB

KOORC

Mar 6, 2003

34. Document ID: US 20030042308 A1

PGPUB-DOCUMENT-NUMBER: 20030042308

PGPUB-FILING-TYPE: new

L19: Entry 34 of 84

DOCUMENT-IDENTIFIER: US 20030042308 A1

TITLE: Pliim-based semiconductor chips

PUBLICATION-DATE: March 6, 2003

NAME	CITY	STATE	COUNTRY	RULE-47
Tsikos, Constantine J.	Voorhees	NJ	US	
Wirth, Allan	Bedford	MA	US	
Good, Timothy A.	Clementon	NJ	US	
Jankevics, Andrew	Westford	MA	US	
Kim, Steve Y.	Cambridge	MA	US	
Amundsen, Thomas	Turnersville	NJ	US	
Naylor, Charles A.	Sewell	NJ	US	
Dobbs, Russell Joseph	Cherry Hill	NJ	US	
Giordano, Patrick A.	Black wood	NJ	US	
Yorsz, Jeffery	Winchester	MA	US	
Schmidt, Mark S.	Williamstown	NJ	US	
Colavito, Stephen J.	Brookhaven	PA	US	
Wilz, David M.	Sewell	NJ	US	
Au, Ka Man	Philadelphia	PA	US	
Svedas, William	Deptford	NJ	US	
Ghosh, Sankar	Glenolden	PA	US	
Schnee, Michael D.	Aston	PA	US	
Zhu, Xiaoxun	Marlton	NJ	US	
Knowles, C. Harry	Moorestown	NJ	US	

US-CL-CURRENT: 235/454

Title Citation Front Review Classification Date Reference Sequences Attachments

KWC

35. Document ID: US 20030042304 A1

L19: Entry 35 of 84

File: PGPB

Mar 6, 2003

PGPUB-DOCUMENT-NUMBER: 20030042304

PGPUB-FILING-TYPE: new

DOCUMENT-IDENTIFIER: US 20030042304 A1

TITLE: Automatic vehicle identification and classification (AVIC) system employing a

tunnel-arrangement of PLIIM-based subsystems

PUBLICATION-DATE: March 6, 2003

INVENTOR-INFORMATION:

NAME

CITY

STATE

COUNTRY

RULE-47

Knowles, C. Harry

Moorestown

NJ

Zhu, Xiaoxun

Marlton

NJ

US US

Schnee, Michael D.

Aston

PΆ US

US-CL-CURRENT: 235/384

Full Title Citation Front Review Classification Date Reference Sequences Attachments Draw Desc Image

EXMC

36. Document ID: US 20030042303 A1

L19: Entry 36 of 84

File: PGPB

Mar 6, 2003

PGPUB-DOCUMENT-NUMBER: 20030042303

PGPUB-FILING-TYPE: new

DOCUMENT-IDENTIFIER: US 20030042303 A1

TITLE: Automatic vehicle identification (AVI) system employing planar laser

illumination imaging (PLIIM) based subsystems

PUBLICATION-DATE: March 6, 2003

INVENTOR-INFORMATION:

NAME Tsikos, Constantine J.

Knowles, C. Harry Zhu, Xiaoxun

Schnee, Michael D.

CITY

Voorhees Moorestown STATE COUNTRY US NJ NJ US

RULE-47

Marlton Aston

NJ PΑ

US US

US-CL-CURRENT: 235/384

Full Title Citation Front Review Classification Date Reference Sequences Attachments

Drawk Desc | Image

37. Document ID: US 20030038179 A1

L19: Entry 37 of 84

File: PGPB

Feb 27, 2003

PGPUB-DOCUMENT-NUMBER: 20030038179

PGPUB-FILING-TYPE: new

DOCUMENT-IDENTIFIER: US 20030038179 A1

TITLE: Tunnel-based method of and system for identifying transported packages employing the transmission of package dimension data over a data communications network and the transformation of package dimension data at linear <u>imaging</u> subsystems in said tunnel-based system so as to enable the control of auto zoom/focus camera modules therewithin during linear imaging operations

PUBLICATION-DATE: February 27, 2003

INVENTOR-INFORMATION:

NAME	CITY	STATE	COUNTRY	RULE-47
Tsikos, Contantine J.	Voorhees	ПЛ	US	
Knowles, C. Harry	Moorestown	NJ	US	
Zhu, Xiaoxun	Marlton	ПJ	US	
Au, Ka Man	Philadelphia	PA	US	
Ghosh, Sankar	Glenolden	PA	US	

US-CL-CURRENT: 235/454

Full Title Citation Front Review Classification Date Reference Sequences Affachments
Draw Descriptings

KMAC

38. Document ID: US 20030035461 A1

L19: Entry 38 of 84

File: PGPB

Feb 20, 2003

PGPUB-DOCUMENT-NUMBER: 20030035461

PGPUB-FILING-TYPE: new

DOCUMENT-IDENTIFIER: US 20030035461 A1

TITLE: Hand-supportable planar laser illumination and imaging (PLIIM) device employing a pair of linear laser diode arrays mounted about a linear image detection array, for illuminating an object to be imaged with a plurality of optically-combined spatially-incoherent planar laser illumination beams (PLIBS) and reducing the speckle-pattern noise power in detected linear images by temporally-averaging detected speckle-noise patterns during the photo-integration time period of said linear image detection array

PUBLICATION-DATE: February 20, 2003

INVENTOR-INFORMATION:

NAME	CITY	STATE	COUNTRY	RULE-47
Tsikos, Constantine J.	Voorhees	NJ	US	
Knowles, C. Harry	Moorestown	NJ	US	
Schnee, Michael D.	Aston	PA	US	
Good, Timothy A.	Clementon	NJ	US	

US-CL-CURRENT: 372/108; 372/43

KWIC

39. Document ID: US 20030035460 A1

L19: Entry 39 of 84

File: PGPB

Feb 20, 2003

PGPUB-DOCUMENT-NUMBER: 20030035460

PGPUB-FILING-TYPE: new

DOCUMENT-IDENTIFIER: US 20030035460 A1

TITLE: Planar laser illumination and imaging (PLIIM) device employing a linear image detection array having vertically-elongated image detection elements, wherein the height of the vertically-elongated image detection elements and the F/# parameter of the image formation optics are configured to reduce speckle-pattern noise power through spatial-averaging of detected speckle-noise patterns

PUBLICATION-DATE: February 20, 2003

INVENTOR-INFORMATION:

NAME CITY STATE COUNTRY RULE-47 Tsikos, Constantine J. Voorhees N.T US Knowles, C. Harry Moorestown NJ US Good, Timothy A. Clementon NJ US Giordano, Patrick A. US Blackwood NJ

US-CL-CURRENT: 372/101; 372/43

Full Title Citation Front Review Classification Date Reference Sequences Attachments Draw Desc Image

KWC

40. Document ID: US 20030034396 A1

L19: Entry 40 of 84

File: PGPB

Feb 20, 2003

PGPUB-DOCUMENT-NUMBER: 20030034396

PGPUB-FILING-TYPE: new

DOCUMENT-IDENTIFIER: US 20030034396 A1

TITLE: Method of speckle-noise pattern reduction and apparatus therefor based on reducing the spatial-coherence of the planar laser illumination beam before it illuminates the target object by applying spatial phase modulation techniques during the transmission of the PLIB towards the target

PUBLICATION-DATE: February 20, 2003

INVENTOR-INFORMATION:

NAME CITY STATE COUNTRY RULE-47 Tsikos, Constantine J. Voorhees US NJ Knowles, C. Harry Moorestown NJ US Wirth, Allan Bedford MA US Good, Timothy A. Clementon US NJ US Jankevics, Andrew Westford MA

US-CL-CURRENT: 235/454



KVMC

41. Document ID: US 20030034395 A1

L19: Entry 41 of 84

File: PGPB

Feb 20, 2003

PGPUB-DOCUMENT-NUMBER: 20030034395

PGPUB-FILING-TYPE: new

DOCUMENT-IDENTIFIER: US 20030034395 A1

TITLE: Planar light illumination and $\underline{imaging}$ (PLIIM) based system having a linear \underline{image} detection chip mounting assembly with means for preventing misalignment between the field of view (\underline{FOV}) of said linear \underline{image} detection chip and the co-planar laser illumination beam (PLIB) produced by said PLIIM based system, in response to thermal expansion and/or contraction within said PLIIM based system

PUBLICATION-DATE: February 20, 2003

INVENTOR-INFORMATION:

NAME	CITY	STATE	COUNTRY R	ULE-47
Tsikos, Constantine J.	Voorhees	NJ	US	
Knowles, C. Harry	Moorestown	NJ	US	
Zhu, Xiaoxun	Marlton	NJ	US	
Schnee, Michael D.	Aston	PA	US	
Au, Ka Man	Philadelphia	PA	US	
Wirth, Allan	Bedford	MA	US	
Good, Timothy A.	Clementon	NJ	US	
Jankevics, Andrew	Westford	MA	US	
Ghosh, Sankar	Glenolden	PA	US	
Naylor, Charles A.	Sewell	NJ	US	
Amundsen, Thomas	Turnersville	NJ	US	
Blake, Robert	Woodbury Heights	NJ	US	
Svedas, William	Deptford	NJ	US	
Defoney, Shawn	Runnemede	NJ	US	
Skypala, Edward	Blackwood	NJ	US	
Vatan, Pirooz	Wilmington	MA	US	
Dobbs, Russell Joseph	Cherry Hill	NJ	US	
Kolis, George	Pennsauken	NJ	US	
Schmidt, Mark C.	Williamstown	NJ	US	
Yorsz, Jeffery	Winchester	MA	US	
Giordano, Patrick A.	Blackwood	NJ	US	
Colavito, Stephen J.	Brookhaven	PA	US	
Wilz,, David W. SR.	Sewell	NJ	US	
Schwartz, Barry E.	Haddonfield	NJ	US	
Kim, Steven Y.	Cambridge	MA	US	
Fisher, Dale	Voorhees	NJ	US	
Tassell, Jon Van	Winchester	MA	US	

US-CL-CURRENT: 235/454

KWC

42. Document ID: US 20030034387 A1

L19: Entry 42 of 84

File: PGPB

Feb 20, 2003

PGPUB-DOCUMENT-NUMBER: 20030034387

PGPUB-FILING-TYPE: new

DOCUMENT-IDENTIFIER: US 20030034387 A1

TITLE: Object identification and attribute information acquisition and linking

computer system

PUBLICATION-DATE: February 20, 2003

INVENTOR-INFORMATION:

NAME CITY STATE COUNTRY RULE-47 Knowles, C. Harry Moorestown NJ US Ghosh, Sankar Glenolden PA US Defoney, Shawn Runnemede NJ US Skypala, Edward Blackwood NJ US Schmidt, Mark C. Williamstown N.T US

US-CL-CURRENT: 235/375

Full | Title | Citation | Front | Review | Classification | Date | Reference | Sequences | Attachments | Draw Desc | Image | F.NUR

3. Document ID: US 20030024987 A1

L19: Entry 43 of 84

File: PGPB

Feb 6, 2003

PGPUB-DOCUMENT-NUMBER: 20030024987

PGPUB-FILING-TYPE: new

DOCUMENT-IDENTIFIER: US 20030024987 A1

TITLE: Method of and apparatus for producing a digital <u>image</u> of an object with reduced speckle-patternnoise, by consecutively capturing, buffering and <u>processing</u> a series of digital <u>images</u> of the object over a series of consecutively different

photo-integration time periods

PUBLICATION-DATE: February 6, 2003

INVENTOR-INFORMATION:

NAME CITY

CITY STATE COUNTRY

Zhu, Xiaoxun Marlton NJ US

US-CL-CURRENT: 235/454

Full Title Citation Front Review Classification Date Reference Sequences Affachments

Kiline

RULE-47

Drawk Desc - Image

44. Document ID: US 20030019933 A1

L19: Entry 44 of 84

File: PGPB

Jan 30, 2003

PGPUB-DOCUMENT-NUMBER: 20030019933

PGPUB-FILING-TYPE: new

DOCUMENT-IDENTIFIER: US 20030019933 A1

TITLE: Automated object identification and attribute acquisition system having a multi-compartment housing with optically-isolated light transmission apertures for operation of a planar laser illumination and imaging (PLIIM) based linear imaging subsystem and a laser-based object profiling subsystem integrated therein

PUBLICATION-DATE: January 30, 2003

INVENTOR-INFORMATION:

NAME	CITY	STATE	COUNTRY	RULE-47
Tsikos, Constantine J.	Voorhees	NJ	US	
Knowles, C. Harry	Moorestown	NJ	US	
Zhu, Xiaoxun	Marlton	NJ	US	
Schnee, Michael D.	Aston	PA	US	
Naylor, Charles A.	Sewell	NJ	US	
Amundsen, Thomas	Turnersville	NJ	US	
Dobbs, Russell Joseph	Cherry Hill	NJ	US	

US-CL-CURRENT: 235/454

Full | Title | Citation | Front | Review | Classification | Date | Reference | Sequences | Attachments | Draw Desc | Image |

KIMC

45. Document ID: US 20030019932 A1

L19: Entry 45 of 84

File: PGPB

Jan 30, 2003

PGPUB-DOCUMENT-NUMBER: 20030019932

PGPUB-FILING-TYPE: new

DOCUMENT-IDENTIFIER: US 20030019932 A1

TITLE: Method of speckle-noise pattern reduction and <u>apparatus</u> therefor based on reducing the temporal-coherence of the planar laser illumination beam before it illuminates the target object by applying temporal frequency modulation techniques during the transmission of the PLIB towards the target

PUBLICATION-DATE: January 30, 2003

INVENTOR-INFORMATION:

NAME	CITY	STATE	COUNTRY	RULE-47
Tsikos, Constantine J.	Voorhees	NJ	US	
Knowles, C. Harry	Moorestown	NJ	US	
Wirth, Allan	Bedford	MA	US	
Good, Timothy A.	Clementon	NJ	US	
Jankevics, Andrew	Westford	MA	US	

US-CL-CURRENT: 235/454

Full Title Citation Front Review Classification Date Reference Sequences Attachments

Draw Desc Image

KWC

46. Document ID: US 20030019931 A1

L19: Entry 46 of 84

File: PGPB

Jan 30, 2003

PGPUB-DOCUMENT-NUMBER: 20030019931

PGPUB-FILING-TYPE: new

DOCUMENT-IDENTIFIER: US 20030019931 A1

TITLE: Method of speckle-noise pattern reduction and <u>apparatus</u> therefor based on reducing the temporal-coherence of the planar laser illumination beam (PLIB) after it illuminates the target by applying temoporal intensity modulation techniques during the detection of the reflected/scattered PLIB

PUBLICATION-DATE: January 30, 2003

INVENTOR - INFORMATION:

CITY STATE COUNTRY RULE-47 NAME Tsikos, Constantine J. Voorhees NJ US NJ US Knowles, C. Harry Moorestown Bedford MA US Wirth, Allan US Clementon NJ Good, Timothy A. US Jankevics, Andrew Wesford MA

US-CL-CURRENT: 235/454

Full Title Citation Front Review Classification Date Reference Sequences Attachments

Draw Desc Image

KUMC

47. Document ID: US 20030011369 A1

L19: Entry 47 of 84

File: PGPB

Jan 16, 2003

PGPUB-DOCUMENT-NUMBER: 20030011369

PGPUB-FILING-TYPE: new

DOCUMENT-IDENTIFIER: US 20030011369 A1

TITLE: Moving table MRI with frequency $\underline{\text{-encoding}}$ in the z $\underline{\text{-direction}}$

PUBLICATION-DATE: January 16, 2003

INVENTOR-INFORMATION:

NAME CITY STATE COUNTRY RULE-47

Brittain, Jean H. Palo Alto CA US
Pauly, John M. Redwood City CA US

US-CL-CURRENT: 324/309; 324/307, 324/318

Full Title Citation Front Review Classification Date Reference Sequences Affachments

KOMC

Draw Deso Image

48. Document ID: US 20020195496 A1

L19: Entry 48 of 84

File: PGPB

Dec 26, 2002

PGPUB-DOCUMENT-NUMBER: 20020195496

PGPUB-FILING-TYPE: new

DOCUMENT-IDENTIFIER: US 20020195496 A1

TITLE: Planar LED-based illumination array (PLIA) chips

PUBLICATION-DATE: December 26, 2002

INVENTOR-INFORMATION:

NAME CITY STATE COUNTRY RULE-47

Tsikos, Constantine J. Voorhees NJ US Good, Timothy A. Clementon NJ US Turnersville US Amundsen, Thomas NJ Knowles, C. Harry NJ US Moorestown

US-CL-CURRENT: 235/462.01

Full Title Citation Front Review Classification Date Reference Sequences Attachments Draw Desc Image E000C

49. Document ID: US 20020186870 A1

L19: Entry 49 of 84

File: PGPB

Dec 12, 2002

PGPUB-DOCUMENT-NUMBER: 20020186870

PGPUB-FILING-TYPE: new

DOCUMENT-IDENTIFIER: US 20020186870 A1

TITLE: Automatic coil selection of multi-receiver MR data using fast prescan data

analysis

PUBLICATION-DATE: December 12, 2002

INVENTOR-INFORMATION:

NAME CITY STATE COUNTRY RULE-47

Ma, Jingfei Waukesha WI US Tan, Guosheng Waukesha WI US

US-CL-CURRENT: 382/131; 382/282

Full Title Citation Front Review Classification Date Reference Sequences Attachments

Draw Desc Image:

KONC

•

50. Document ID: US 20020181753 A1

L19: Entry 50 of 84 File: PGPB Dec 5, 2002

PGPUB-DOCUMENT-NUMBER: 20020181753

PGPUB-FILING-TYPE: new

DOCUMENT-IDENTIFIER: US 20020181753 A1

28 of 45

TITLE: Adaptive data differentiation and selection from multi-coil receiver to

reduce artifacts in reconstruction

PUBLICATION-DATE: December 5, 2002

INVENTOR-INFORMATION:

NAME

CITY

STATE

COUNTRY

RULE-47

Ma, Jingfei

Waukesha

WI

US

Tan, Guosheng

Waukesha

WI

US

US-CL-CURRENT: 382/131

Full | Title | Citation | Front | Review | Classification | Date | Reference | Sequences | Attachments | Draw Deso | Image |

Kiint

51. Document ID: US 20020177770 A1

L19: Entry 51 of 84

File: PGPB

Nov 28, 2002

PGPUB-DOCUMENT-NUMBER: 20020177770

PGPUB-FILING-TYPE: new

DOCUMENT-IDENTIFIER: US 20020177770 A1

TITLE: Assessing the condition of a joint and assessing cartilage loss

PUBLICATION-DATE: November 28, 2002

INVENTOR-INFORMATION:

NAME

CITY

STATE

COUNTRY

RULE-47

Lang, Philipp Steines, Daniel Lexington Palo Alto

MA CA US US

US-CL-CURRENT: 600/410

Full | Title | Citation | Front | Review | Classification | Date | Reference | Sequences | Attachments | Draw Desc | Image |

KWC

52. Document ID: US 20020173715 A1

L19: Entry 52 of 84

File: PGPB

Nov 21, 2002

PGPUB-DOCUMENT-NUMBER: 20020173715

PGPUB-FILING-TYPE: new

DOCUMENT-IDENTIFIER: US 20020173715 A1

TITLE: Method for acquiring MRI data from a large field of view using continuous

table motion

PUBLICATION-DATE: November 21, 2002

INVENTOR-INFORMATION:

NAME

CITY

STATE COUNTRY

RULE-47

Kruger, David G.

WI

Riederer, Stephen J.

Nelson Rochester

MN

US US US-CL-CURRENT: 600/410

Full Title Citation Front Review Classification Date Reference Sequences Attachments

Draw Desc Image

KWC

53. Document ID: US 20020153422 A1

L19: Entry 53 of 84

File: PGPB

Oct 24, 2002

RULE-47

PGPUB-DOCUMENT-NUMBER: 20020153422

PGPUB-FILING-TYPE: new

DOCUMENT-IDENTIFIER: US 20020153422 A1

TITLE: Planar led-based illumination modules

PUBLICATION-DATE: October 24, 2002

INVENTOR-INFORMATION:

NAME	CITY	STATE	COUNTRY
Tsikos, Constantine J.	Voorhees	NJ	US
Wirth, Allan	Bedford	MA	US
Good, Timothy A.	Clementon	NJ	US
Jankevics, Andrew	Westford	MA	US
Kim, Steve Y.	Cambridge	MA	US
Amundsen, Thomas	Turnersville	NJ	US
Naylor, Charles A.	Sewell	NJ	US
Dobbs, Russell Joseph	Cherry Hill	NJ	US
Giordano, Patrick A.	Blackwood	NJ	US
Yorsz, Jeffery	Winchester	MA	US
Schmidt, Mark S.	Williamstown	NJ	US
Colavito, <u>Stephen</u> J.	Brookhaven	PA	US
Wilz, David M. SR.	Sewell	NJ	US
Au, Ka Man	Philadelphia	PA	US
Svedas, William	Deptford	NJ	US
Ghosh, Sankar	Glenolden	PA	US
Schnee, Michael D.	Aston	PA	US
Zhu, Xiaoxun	Marlton	NJ	US
Knowles, C. Harry	Moorestown	NJ	US

a====

US-CL-CURRENT: 235/454

Full Title Citation Front Review Classification Date Reference Sequences Attachments
Draw Descriptings

X(0)

54. Document ID: US 20020145042 A1

L19: Entry 54 of 84

File: PGPB

Oct 10, 2002

PGPUB-DOCUMENT-NUMBER: 20020145042

PGPUB-FILING-TYPE: new

DOCUMENT-IDENTIFIER: US 20020145042 A1

TITLE: Internet-based remote monitoring, configuration and service (RMCS) system

capable of monitoring, configuring and servicing a planar laser illumination and

PUBLICATION-DATE: October 10, 2002

imaging (PLIIM) based network

INVENTOR-INFORMATION:

NAME	CITY	STATE	COUNTRY	RULE-47
Knowles, C. Harry	Moorestown	NJ	US	
Schmidt, Mark C.	Williamstown	NJ	US	
Zhu, Xiaoxun	Marlton	NJ	US	
Defoney, Shawn	Runnemede	NJ	US	
Skypala, Edward	Blackwood	NJ	US	
Tsikos, Constantine J.	Voorhees	NJ	US	
Au, Ka Man	Philadelphia	PA	US	
Schwartz, Barry E.	Haddonfield	NJ	US	
Wirth, Allan	Bedford	MA	US	
Jankevics, Andrew	Westford	MA	US	
Good, Timothy A.	Clementon	NJ	US	
Ghosh, Sankar	Glenolden	PA	US	
Schnee, Michael D.	Aston	PA	US	
Kolis, George	Pennsauken	NJ	US	
Amundsen, Thomas	Turnersville	NJ	US	
Naylor, Charles A.	Sewell	NJ	US	
Blake, Robert	Woodbury Heights	NJ	US	
Dobbs, Russell Joseph	Cherry Hill	NJ	US	
Yorsz, Jeffery	Winchester	MA	US	
Giordano, Patrick A.	Blackwood	NJ	US	
Colavito, <u>Stephen</u> J.	Brookhaven	PA	US	
Wilz, David W. SR.	Sewell	NJ	US	
Svedas, William	Deptford	NJ	US	
Kim, Steven Y.	Cambridge	MA	US	
Fischer, Dale M.	Voorhees	NJ	US	
Tassell, Jon Van	Winchester	MA	US	

US-CL-CURRENT: 235/462.01

Full Title Citation Front Review Classification Date Reference Sequences Attachments	KUMC
Draw Desc Image	

55. Document ID: US 20020143247 A1

L19: Entry 55 of 84 File: PGPB Oct 3, 2002

PGPUB-DOCUMENT-NUMBER: 20020143247

PGPUB-FILING-TYPE: new

DOCUMENT-IDENTIFIER: US 20020143247 A1

TITLE: Method and apparatus of acquiring large FOV images without slab-boundary

artifacts

PUBLICATION-DATE: October 3, 2002

NAME

Pauly, John Mark

CITY

STATE COUNTRY

US

RULE-47

Brittain, Jean Helen

Pewaukee

Redwood City

WI CA

US

US-CL-CURRENT: 600/410

Full Title Citation Front Review Classification Date Reference Sequences Attachments

Draw Descriptings

......

KURC

56. Document ID: US 20020140423 A1

L19: Entry 56 of 84

File: PGPB

Oct 3, 2002

PGPUB-DOCUMENT-NUMBER: 20020140423

PGPUB-FILING-TYPE: new

DOCUMENT-IDENTIFIER: US 20020140423 A1

TITLE: Moving table MRI with frequency -encoding in the z-direction

PUBLICATION-DATE: October 3, 2002

INVENTOR-INFORMATION:

NAME

CITY

STATE

COUNTRY

RULE-47

Brittain, Jean Helen

Menlo Park

CA

US

US-CL-CURRENT: 324/301; 324/309

Full Title Citation Front Review Classification Date Reference Sequences Attachments Draw Desc Image KIMC

57. Document ID: US 20020139853 A1

L19: Entry 57 of 84

File: PGPB

Oct 3, 2002

PGPUB-DOCUMENT-NUMBER: 20020139853

PGPUB-FILING-TYPE: new

DOCUMENT-IDENTIFIER: US 20020139853 A1

TITLE: Planar laser illumination and $\underline{imaging}$ (PLIIM) system employing wavefront control methods forreducing the power of speckle-pattern noise digital \underline{images}

acquired by said system

PUBLICATION-DATE: October 3, 2002

NAME	CITY	STATE	COUNTRY	RULE-47
Tsikos, Constantine J.	Voorhees	NJ	US	
Wirth, Allan	Bedford	MA	US	
Good, Timothy A.	Clementon	NJ	US	•
Jankevics, Andrew	Westford	MA	US	
Kim, Steve Y.	Cambridge	MA	US	
Amundsen, Thomas	Turnersville	NJ	US	
Naylor, Charles A.	Sewell	NJ	US	
Dobbs, Russell Joseph	Cherry Hill	NJ	US	
Giordano, Patrick A.	Blackwood	NJ	US	
Yorsz, Jeffery	Winchester	MA	US	
Schmidt, Mark S.	Williamstown	NJ	US	
Colavito, <u>Stephen</u> J.	Brookhaven	PA	US	
Wilz, David M. SR.	Sewell	NJ	US	
Au, Ka Man	Philadelphia	PA	US	
Svedas, William	Deptford	NJ	US	
Ghosh, Sankar	Glenolden	PA	US	
Schnee, Michael D.	Aston	PA	US	
Zhu, Xiaoxun	Marlton	NJ	US	
Knowles, C. Harry	Moorestown	NJ	US	

US-CL-CURRENT: 235/462.01

Full Title Citation Front Review Classification Date Reference Sequences Attachments	KUMC
Draw Deso Image	

......

58. Document ID: US 20020101568 A1

L19: Entry 58 of 84

File: PGPB

Aug 1, 2002

PGPUB-DOCUMENT-NUMBER: 20020101568

PGPUB-FILING-TYPE: new

DOCUMENT-IDENTIFIER: US 20020101568 A1

TITLE: Interactive data view and command system

PUBLICATION-DATE: August 1, 2002

INVENTOR-INFORMATION:

NAME	CITY	STATE	COUNTRY	RULE-47
Eberl, Heinrich A.	Probstried		DE	
Eberl, Roland H.C.	Munchen		DE	
Dickerson, David P.	Freising		DE	
Konigstein, Karsten	Seefeld		DE	
Jochheim, <u>Edgar</u>	Munchen		DE	

US-CL-CURRENT: 351/211; 351/206

Full Title Cit	ition Front Revie	ω Classification D	ate Reference Sequ	iences Attachments	KIME
Draint Descriptions					

59. Document ID: US 20020087274 A1

L19: Entry 59 of 84

File: PGPB

Jul 4, 2002

PGPUB-DOCUMENT-NUMBER: 20020087274

PGPUB-FILING-TYPE: new

DOCUMENT-IDENTIFIER: US 20020087274 A1

TITLE: Assessing the condition of a joint and preventing damage

PUBLICATION-DATE: July 4, 2002

INVENTOR-INFORMATION:

NAME CITY STATE COUNTRY RULE-47

Alexander, Eugene J. San Francisco CA US CA US Andriacchi, Thomas P. Los Altos Hills San Francisco CA US Lang, Philipp Napel, Sandy A. Menlo Park CA US

US-CL-CURRENT: 702/19; 378/3

Full Title Citation Front Review Classification Date Reference Sequences Attachments.

Draw Desc Image

KOMO

60. Document ID: US 20020068865 A1

L19: Entry 60 of 84 File: PGPB Jun 6, 2002

PGPUB-DOCUMENT-NUMBER: 20020068865

PGPUB-FILING-TYPE: new

DOCUMENT-IDENTIFIER: US 20020068865 A1

TITLE: Method and apparatus for magnetic resonance arteriography using contrast

agents

PUBLICATION-DATE: June 6, 2002

INVENTOR-INFORMATION:

NAME CITY STATE COUNTRY RULE-47

Meaney, James F.M. Leeds MI GB Prince, Martin R. Ann Arbor US

US-CL-CURRENT: 600/415; 600/420

Full | Title | Citation | Front | Review | Classification | Date | Reference | Sequences | Attachments | Draw Desc | Image | KOME

61. Document ID: US 20020064341 A1

L19: Entry 61 of 84 File: PGPB May 30, 2002

PGPUB-DOCUMENT-NUMBER: 20020064341

PGPUB-FILING-TYPE: new

DOCUMENT-IDENTIFIER: US 20020064341 A1

10/27/2003 9:15 AM

TITLE: Micro-fabricated optical waveguide for use in scanning fiber displays and

scanned fiber image acquisition

PUBLICATION-DATE: May 30, 2002

INVENTOR - INFORMATION:

NAME CITY STATE COUNTRY RULE-47 Fauver, Mark E. Seattle WA US Seibel, Eric J. WA US Seattle Brown, Chris M. Seattle WA US Reinhall, Per G. Seattle WA US Smithwick, Quinn Y.J. Bothell WA US

US-CL-CURRENT: 385/25; 359/209, 385/43

Full Title Citation Front Review Classification Date Reference Sequences Attachments KMC Draw Desc Image

62. Document ID: US 20020043561 A1

L19: Entry 62 of 84

File: PGPB

Apr 18, 2002

PGPUB-DOCUMENT-NUMBER: 20020043561

PGPUB-FILING-TYPE: new

DOCUMENT-IDENTIFIER: US 20020043561 A1

TITLE: Method of and system for producing digital <u>images</u> of objects with subtantially reduced speckle-noise patterns by illuminating said objects with spatially and/or temporally coherent-reduced planar laser illumination

PUBLICATION-DATE: April 18, 2002

INVENTOR-INFORMATION:

CITY COUNTRY NAME STATE RULE-47 Voorhees NJ US Tsikos, Constantine J. Bedford MA US Wirth, Allan Westford MA US Jankevics, Andrew US Kim, Steve Y. Cambridge MA Good, Timothy Clementon ŊJ US Amundsen, Thomas Turnersville NJ US Sewell Naylor, Charles A. ΝJ US Dobbs, Russell Joseph Cherry Hill ΝĴ US Zhu, Xiaoxun Marlton NJ US PA Schnee, Michael D. Aston US Knowles, Carl Harry US Moorestown NJ

US-CL-CURRENT: 235/454; 257/E21.172, 257/E29.144

Full | Title | Citation | Front | Review | Classification | Date | Reference | Sequences | Attachments | Draw Desc | Image |

KUNC

63. Document ID: US 20020013526 A1

L19: Entry 63 of 84

File: PGPB

Jan 31, 2002

PGPUB-DOCUMENT-NUMBER: 20020013526

PGPUB-FILING-TYPE: new

DOCUMENT-IDENTIFIER: US 20020013526 A1

TITLE: Inherently de-coupled sandwiched solenoidal array coil

PUBLICATION-DATE: January 31, 2002

INVENTOR-INFORMATION:

NAME CITY STATE COUNTRY RULE-47

Su, Sunyu South San Francisco CA US
Kaufman, Leon San Francisco CA US
Arakawa, Mitsuaki Hillsborough CA US

US-CL-CURRENT: 600/422; 324/318

Full Title Citation Front Review Classification Date Reference Sequences Attachments.

Draw Desc. Image

KOMC

64. Document ID: US 20010003423 A1

L19: Entry 64 of 84 File: PGPB Jun 14, 2001

PGPUB-DOCUMENT-NUMBER: 20010003423 PGPUB-FILING-TYPE: new-utility

DOCUMENT-IDENTIFIER: US 20010003423 A1

TITLE: Magnetic resonance imaging

PUBLICATION-DATE: June 14, 2001

INVENTOR-INFORMATION:

NAME CITY STATE COUNTRY RULE-47

Wald, Lawrence L. Cambridge MA US

US-CL-CURRENT: 324/307

Full Title Citation Front Review Classification Date Reference Sequences Attachments

Draw Desc Image:

EUNC

65. Document ID: US 6584337 B2

L19: Entry 65 of 84 File: USPT Jun 24, 2003

US-PAT-NO: 6584337

DOCUMENT-IDENTIFIER: US 6584337 B2

TITLE: Method and system for extended volume imaging using MRI

DATE-ISSUED: June 24, 2003

INVENTOR-INFORMATION:

NAME

CITY STATE ZIP CODE

Dumoulin; Charles Lucian

Ballston Lake

COUNTRY

Zhu; Yudong

Clifton Park

NY NY

US-CL-CURRENT: 600/410; 324/309, 600/415

Full Title Citation Front Review Classification Date Reference Sequences Draw Deso Image

KUNC

66. Document ID: US 6567567 B1

L19: Entry 66 of 84

File: USPT

May 20, 2003

US-PAT-NO: 6567567

DOCUMENT-IDENTIFIER: US 6567567 B1

TITLE: Sampling and reconstruction of RF signals

DATE-ISSUED: May 20, 2003

INVENTOR-INFORMATION:

NAME CITY STATE ZIP CODE COUNTRY

Levin; David N. Chicago ILOak Park Nagle; Scott TT

US-CL-CURRENT: 382/284; 382/128

Title Citation Front Review Classification Date Reference Sequences Attachments Draw Desc Image

KOMC

67. Document ID: US 6564085 B2

L19: Entry 67 of 84 File: USPT May 13, 2003

US-PAT-NO: 6564085

DOCUMENT-IDENTIFIER: US 6564085 B2

TITLE: Method and apparatus for magnetic resonance arteriography using contrast

agents

DATE-ISSUED: May 13, 2003

INVENTOR-INFORMATION:

NAME CITY STATE ZIP CODE COUNTRY

Meaney; James F.M. Leeds LS29NS GB

Prince; Martin R. Ann Arbor ΜI 48104

US-CL-CURRENT: 600/415; 324/306, 324/309, 600/420

Title Citation Front Review Classification Date Reference Sequences Attachments

(4)))(0

Draw Desc. Image

5.....

68. Document ID: US 6493572 B1

L19: Entry 68 of 84

File: USPT

Dec 10, 2002

US-PAT-NO: 6493572

DOCUMENT-IDENTIFIER: US 6493572 B1

TITLE: Inherently de-coupled sandwiched solenoidal array coil

DATE-ISSUED: December 10, 2002

INVENTOR-INFORMATION:

NAME CITY STATE ZIP CODE COUNTRY

South San Francisco CA Su; Sunyu CA Kaufman; Leon San Francisco Hillsborough Arakawa; Mitsuaki CA CA Carlson; Joseph W. Kensington

US-CL-CURRENT: 600/422; 324/318, 324/322

Full Title Citation Front Review Classification Date Reference Sequences Attachments Draw Desc Image

69. Document ID: US 6479999 B1

L19: Entry 69 of 84

File: USPT

Nov 12, 2002

US-PAT-NO: 6479999

DOCUMENT-IDENTIFIER: US 6479999 B1

TITLE: Efficiently shielded MRI gradient coil with discretely or continuously

variable field of view

DATE-ISSUED: November 12, 2002

INVENTOR-INFORMATION:

CITY STATE ZIP CODE COUNTRY NAME

DeMeester; Gordon D. Wickliffe OH Morich; Michael A. Mentor OH Highland Heights OH Shvartsman; Shmaryu M.

US-CL-CURRENT: 324/318; 324/309, 324/319

Full Title Citation Front Review Classification Date Reference Sequences Attachments Draw Desc Image

KNINC

70. Document ID: US 6377048 B1

L19: Entry 70 of 84 File: USPT Apr 23, 2002

US-PAT-NO: 6377048

DOCUMENT-IDENTIFIER: US 6377048 B1

TITLE: Magnetic resonance imaging device for operation in external static magnetic

38 of 45 10/27/2003 9:15 AM fields

DATE-ISSUED: April 23, 2002

INVENTOR-INFORMATION:

NAME CITY STATE ZIP CODE COUNTRY

Golan; Erez Tel Aviv IL
Blank; Aharon Kiriat Ono IL
Alexandrowicz; Gil Jerusalem IL

US-CL-CURRENT: 324/318; 324/322

Full Title Citation Front Review Classification Date Reference Sequences Attachments

Draw Desc Image

KORBC

71. Document ID: US 6311085 B1

L19: Entry 71 of 84 File: USPT Oct 30, 2001

US-PAT-NO: 6311085

DOCUMENT-IDENTIFIER: US 6311085 B1

TITLE: Method and apparatus for magnetic resonance arteriography using contrast

agents

DATE-ISSUED: October 30, 2001

INVENTOR-INFORMATION:

NAME CITY STATE ZIP CODE COUNTRY

Meaney; James F. M. Leeds LS29NS GB

Prince; Martin R. Ann Arbor MI 48104

US-CL-CURRENT: 600/420; 324/306, 600/415

Full Title Citation Front Review Classification Date Reference Sequences Attachments

Draw Desc Image

Kinc

72. Document ID: US 6307368 B1

L19: Entry 72 of 84 File: USPT Oct 23, 2001

US-PAT-NO: 6307368

DOCUMENT-IDENTIFIER: US 6307368 B1

TITLE: Linear combination steady-state free precession MRI

DATE-ISSUED: October 23, 2001

INVENTOR-INFORMATION:

NAME CITY STATE ZIP CODE COUNTRY

Vasanawala; Shreyas S. Mountain View CA
Pauly; John M. Redwood City CA
Nishimura; Dwight G. Palo Alto CA

US-CL-CURRENT: 324/309; 324/300, 324/307, 324/311

Full Title Citation Front Review Classification Date Reference Sequences Attachments.

Draw Desc. Image:

Kunt

73. Document ID: US 6289232 B1

L19: Entry 73 of 84

File: USPT

Sep 11, 2001

US-PAT-NO: 6289232

DOCUMENT-IDENTIFIER: US 6289232 B1

TITLE: Coil array autocalibration MR imaging

DATE-ISSUED: September 11, 2001

INVENTOR-INFORMATION:

NAME ·

CITY

STATE ZIP CODE

COUNTRY

Jakob; Peter M.

Griswold; Mark

Brookline Village

MA MA

Sodickson; Daniel K.

Cambridge Brookline

MA

US-CL-CURRENT: 600/410; 324/307, 324/309, 324/318, 324/322, 600/422

Full Title Citation Front Review Classification Date Reference Sequences Attachments

Draw Descriptings

KWAL

74. Document ID: US 6275722 B1

L19: Entry 74 of 84

File: USPT

Aug 14, 2001

US-PAT-NO: 6275722

DOCUMENT-IDENTIFIER: US 6275722 B1

TITLE: Methods and apparatus for magnetic resonance imaging with RF coil sweeping

DATE-ISSUED: August 14, 2001

INVENTOR-INFORMATION:

NAME

CITY

STATE

ZIP CODE

COUNTRY

Martin; Alastair

St. Louis Park

MN

Vaals Van; Joop

Best

NL

US-CL-CURRENT: $\underline{600/410}$; $\underline{324/308}$, $\underline{324/318}$, $\underline{324/322}$, $\underline{600/411}$, $\underline{600/414}$, $\underline{600/422}$, $\underline{600/423}$, $\underline{606/130}$

Full Title Citation Front Review Classification Date Reference Sequences Attachments.

Draws Desc. | Image |

300 C

75. Document ID: US 6230040 B1

L19: Entry 75 of 84

File: USPT

May 8, 2001

US-PAT-NO: 6230040

DOCUMENT-IDENTIFIER: US 6230040 B1

TITLE: Method for performing magnetic resonance angiography with dynamic k-s

k-space

sampling

DATE-ISSUED: May 8, 2001

INVENTOR-INFORMATION:

NAME

CITY

STATE

ZIP CODE

COUNTRY

Wang; Yi

New York

NY

Lee; Howard M.

Rye

NY

US-CL-CURRENT: 600/415; 324/309

Full Title Citation Front Review Classification Date Reference Sequences Atlachments NMC Draw Desc Image

76. Document ID: US 6181134 B1

L19: Entry 76 of 84

File: USPT

Jan 30, 2001

US-PAT-NO: 6181134

DOCUMENT-IDENTIFIER: US 6181134 B1

TITLE: Magnetic resonance imaging of the distribution of a marker compound without

obtaining spectral information

DATE-ISSUED: January 30, 2001

INVENTOR-INFORMATION:

NAME

CITY

STATE

ZIP CODE

COUNTRY

Wald; Lawrence L.

Cambridge

MA

US-CL-CURRENT: 324/307; 324/309

Full Title Citation Front Review Classification Date Reference Sequences Attachments Fullo Brain Desc Timage

77. Document ID: US 6144873 A

L19: Entry 77 of 84

File: USPT

Nov 7, 2000

US-PAT-NO: 6144873

DOCUMENT-IDENTIFIER: US 6144873 A

TITLE: Method of efficient data encoding in dynamic magnetic resonance imaging

DATE-ISSUED: November 7, 2000

INVENTOR-INFORMATION:

NAME

CITY

STATE

ZIP CODE

COUNTRY

Madore; Bruno

Redwood City

CA

Glover; Gary H.

Stanford

CA

Pelc; Norbert J.

Los Altos

CA

US-CL-CURRENT: 600/410; 324/309

Full Title Citation Front Review Classification Date Reference Sequences Attachments

Draw Desc Image

K0080

78. Document ID: US 6091243 A

L19: Entry 78 of 84

File: USPT

Jul 18, 2000

US-PAT-NO: 6091243

DOCUMENT-IDENTIFIER: US 6091243 A

TITLE: Water-fat imaging with direct phase encoding (DPE)

DATE-ISSUED: July 18, 2000

INVENTOR-INFORMATION:

NAME

CITY

STATE

ZIP CODE

COUNTRY

Xiang; Qing-San

Vancouver

CA

An; Li

Vancouver

CA

US-CL-CURRENT: 324/307; 324/309

Full Title Citation Front Review Classification Date Reference Sequences Attachments

Draw Description

KUME

79. Document ID: US 6018600 A

L19: Entry 79 of 84

File: USPT

Jan 25, 2000

US-PAT-NO: 6018600

DOCUMENT-IDENTIFIER: US 6018600 A

TITLE: Sampling and reconstruction of signals and images including MR images of

multiple regions

DATE-ISSUED: January 25, 2000

INVENTOR-INFORMATION:

NAME

CITY

STATE

ZIP CODE

COUNTRY

Levin; David N.

Nagle; Scott

Chicago Oak Park IL IL

US-CL-CURRENT: 382/284; 382/131

Full | Title | Citation | Front | Review | Classification | Date | Reference | Sequences | Attachments | Draw Cess | Image |

FUNC.

http://westbrs:8002/bin/gate.exe?f=TOC&s...e=LSPT.PGPB.JPAB.EPAB.DWPI.TDBD&ESNAME=-

80. Document ID: US 5928148 A

File: USPT L19: Entry 80 of 84 Jul 27, 1999

US-PAT-NO: 5928148

DOCUMENT-IDENTIFIER: US 5928148 A

TITLE: Method for performing magnetic resonance angiography over a large field of

view using table stepping

DATE-ISSUED: July 27, 1999

INVENTOR-INFORMATION:

NAME CITY STATE ZIP CODE COUNTRY

Wang; Yi New York NY Lee; Howard M. Rye NY Khilnani; Neil M. New York

US-CL-CURRENT: 600/420; 324/306, 600/415

Full Title Citation Front Review Classification Date Reference Sequences Drawi Desc Image

81. Document ID: US 5924987 A

L19: Entry 81 of 84 File: USPT Jul 20, 1999

US-PAT-NO: 5924987

DOCUMENT-IDENTIFIER: US 5924987 A

TITLE: Method and apparatus for magnetic resonance arteriography using contrast

agents

DATE-ISSUED: July 20, 1999

INVENTOR-INFORMATION:

NAME CITY STATE ZIP CODE COUNTRY

Meaney; James F. M. Leeds LS29NS GB

Prince; Martin R. Ann Arbor MI 48104

US-CL-CURRENT: 600/420; 324/306, 600/415

Full Title Citation Front Review Classification Date Reference Sequences Attachments Draw Desc Image

KWC

82. Document ID: US 5786692 A

L19: Entry 82 of 84 File: USPT Jul 28, 1998

US-PAT-NO: 5786692

DOCUMENT-IDENTIFIER: US 5786692 A

TITLE: Line scan diffusion imaging

Record List Display

DATE-ISSUED: July 28, 1998

INVENTOR-INFORMATION:

NAME CITY STATE ZIP CODE COUNTRY

Maier; Stephan E. Brookline MA Gudbjartsson; Hakon Brookline MA

US-CL-CURRENT: 324/307; 324/309

Full Title Citation Front Review Classification Date Reference Sequences Attachments KMC Draw Desc Image

33. Document ID: US 5652513 A

L19: Entry 83 of 84 File: USPT Jul 29, 1997

US-PAT-NO: 5652513

DOCUMENT-IDENTIFIER: US 5652513 A

TITLE: Phase sensitive magnetic resonance technique with integrated gradient profile

and continuous tunable flow

DATE-ISSUED: July 29, 1997

INVENTOR-INFORMATION:

NAME CITY STATE ZIP CODE COUNTRY

Liu; Haiying Euclid OH
Margosian; Paul M. Lakewood OH
Xu; Yansun Willoughby Hills OH

US-CL-CURRENT: 324/306; 324/309

Full | Title | Citation | Front | Review | Classification | Date | Reference | Sequences | Attachments | Draw Desc | Image |

KIMIC

84. Document ID: US 4209853 A

L19: Entry 84 of 84 File: USPT Jun 24, 1980

US-PAT-NO: 4209853

DOCUMENT-IDENTIFIER: US 4209853 A

TITLE: Holographic system for object location and identification

DATE-ISSUED: June 24, 1980

INVENTOR-INFORMATION:

NAME CITY STATE ZIP CODE COUNTRY

Hyatt; Gilbert P. Anaheim CA 92803

US-CL-CURRENT: 367/8; 342/179, 367/103, 367/11, 367/123, 367/9

Print





Generate Collection

Term	Documents
BEST	930582
BESTS	153
OPTIM\$9	0
OPTIM	119
OPTIMA	2726
OPTIMAAL	3
OPTIMAB	2
OPTIMABILITY	2
OPTIMABLE	2
OPTIMABLY	1
"OPTIMAB.RTM"	5
(L17 AND ((OPTIM\$9 OR IDEAL\$5 OR BEST) WITH (IMAG\$6))).USPT,PGPB,JPAB,EPAB,DWPI,TDBD.	84

There are more results than shown above. Click here to view the entire set.

Display Format: - Change Format

Previous Page Next Page

45 of 45 10/27/2003 9:15 AM

III EST

Generate Collection

Print

L19: Entry 5 of 84

File: PGPB

Jul 17, 2003

PGPUB-DOCUMENT-NUMBER: 20030135111

PGPUB-FILING-TYPE: new

DOCUMENT-IDENTIFIER: US 20030135111 A1

TITLE: Method and apparatus for magnetic resonance arteriography using contrast

agents

PUBLICATION-DATE: July 17, 2003

INVENTOR-INFORMATION:

NAME

CITY

STATE

COUNTRY

RULE-47

Meaney, James F.M.

Leeds

ΜI

GB

Prince, Martin R.

Ann Arbor

US

APPL-NO: 10/ 350487 [PALM]
DATE FILED: January 24, 2003

RELATED-US-APPL-DATA:

Application 10/350487 is a continuation-of US application 10/032860, filed October 23, 2001, US Patent No. 6564085

Application 10/032860 is a continuation-of US application 09/309311, filed May 11,

1999, US Patent No. 6311085

Application 09/309311 is a continuation-of US application 08/944426, filed October 6, 1997, US Patent No. 5924987

INT-CL: [07] A61 B 5/055

US-CL-PUBLISHED: 600/422 US-CL-CURRENT: 600/422

REPRESENTATIVE-FIGURES: 8A

ABSTRACT:

The present invention is a technique of, and system for, imaging vascular anatomy over distance considerably greater than the maximum practical field of view of a magnetic resonance imaging system while using substantially one contrast agent injection. The technique and system of the present invention acquires image data of a plurality of image volumes which are representative of different portions of the patient's body. The image data of each image volume includes image data which is representative of the center of k-space. The acquisition of image data which is representative of the center of k-space is correlated with a concentration of contrast agent in the artery(ies) residing in the image volume being substantially greater than the concentration of contrast agent in veins and background tissue adjacent to the artery(ies). This provides preferential enhancement of arteries relative to adjacent veins and background tissue for each acquisition, wherein each acquisition is representative of a different portion of the arterial system (e.g., abdominal aorta, femoral, popliteal, and tibial arteries).

Nov 21, 2002

M = 3 T

File: PGPB

Generate Collection Print

PGPUB-DOCUMENT-NUMBER: 20020173715

PGPUB-FILING-TYPE: new

L19: Entry 52 of 84

DOCUMENT-IDENTIFIER: US 20020173715 A1

TITLE: Method for acquiring MRI data from a large field of view using continuous

table motion

PUBLICATION-DATE: November 21, 2002

INVENTOR-INFORMATION:

NAME CITY STATE COUNTRY RULE-47

Kruger, David G. Nelson WI US Riederer, Stephen J. Rochester MN US

APPL-NO: 09/ 993120 [PALM]
DATE FILED: November 26, 2001

RELATED-US-APPL-DATA:

Application is a non-provisional-of-provisional application 60/282555, filed April 9, 2001,

INT-CL: [07] A61 B 5/05

US-CL-PUBLISHED: 600/410 US-CL-CURRENT: 600/410

REPRESENTATIVE-FIGURES: 1

ABSTRACT:

MRA data is acquired from a large region of interest by translating the patient through the bore of the MRI system as a three-dimensional MRA data $\underline{\text{set}}$ are acquired. Patient table movement is controlled to track a bolus of contrast agent as it passes through the region of interest. Fluoroscopic $\underline{\text{images}}$ may be acquired during the $\underline{\text{scan}}$ to enable accurate bolus tracking. A seamless $\underline{\text{image}}$ of the entire region of interest is reconstructed.

CROSS-REFERENCE TO RELATED APPLICATIONS

[0001] This application is based on U.S. Provisional Patent Application Serial No. 60/282,555 filed on Apr. 9, 2001 and entitled "Method For Acquiring MRI Data From A Large Field Of View Using Continuous Table Motion."

Generate Collection

Print

L19: Entry 79 of 84

File: USPT

Jan 25, 2000

DOCUMENT-IDENTIFIER: US 6018600 A

TITLE: Sampling and reconstruction of signals and <u>images</u> including MR <u>images</u> of

multiple regions

Abstract Text (1):

A method and apparatus are provided for acquiring and reconstructing an method includes the steps of obtaining prior knowledge of the image, possibly by coarse sampling of the <u>image</u> and using the obtained prior knowledge of the image to identify relative locations of structures having relatively high contrast edges. The upon the relative locations of the structures in order to achieve comparable eigenvalues of a reconstruction matrix and sampling the <u>k-space</u> at the prescribed $\underline{k\text{-space}}$ locations to obtain $\underline{k\text{-space}}$ sample data. The $\underline{k\text{-space}}$ sample data are decomposed into background data and edge data. The background data are Fourier transformed to reconstruct a background <u>image</u> component. Similarly, <u>subsets of the</u> edge data are Fourier transformed and the reconstruction matrix is used to form a linear combination of these Fourier transformations in order to reconstruct an edge image component and the edge image image component. Finally, the background component are combined to generate a final image.

Brief Summary Text (2):

The field of the invention relates to sampling and reconstruction of signals and images including MR images of multiple regions.

Brief Summary Text (4):

MICROFICHE APPENDIX I contains one page of microfiche with 51 frames and is a printout of source code for executing steps of an illustrated embodiment of the invention".

Brief Summary Text (5):

MR imaging is most commonly performed with 2D FT or 3D FT techniques, which require only a modest amount of prior knowledge about the object: 1) the object is assumed to be completely contained within a finite field of view (FOV); 2) the image is assumed to be band-limited in frequency space; i.e. its significant power spectrum does not extend beyond some maximum spatial frequency. If these two assumptions are valid, the usual sampling theorem (due to Whittaker, Kotel'nikov, and Shannon, or WKS, (1-4)) states that the <u>image</u> can be reconstructed by an inverse FT of a finite number of discrete samples of the <u>image's k-space</u> representation. The spacing between the sampled k-space points is determined by the first assumption (the dimensions of the FOV), and the limits of the k-space sampling pattern are determined by the second assumption (the maximum spatial frequencies in the image). This method is widely used because: 1) it is based on relatively weak assumptions about the \underline{image} , 2) it is relatively easy to acquire the Fourier $\underline{-encoded}$ signals stipulated by the WKS theorem, and 3) image reconstruction can be performed efficiently with a fast FT (FFT).

Brief Summary Text (6):

In contrast-enhanced carotid artery <u>imaging</u>, interventional <u>imaging</u>, functional <u>imaging</u>, cardiac <u>imaging</u>, and a number of other applications, the utility of MRI is limited by the speed with which the <u>k-space</u> data can be measured. Two general strategies have been used to shorten <u>image</u> acquisition time. 1) <u>Gradient</u> pulses with shorter rise times and/or larger amplitudes have been used in order to shorten the

time required to gather a <u>complete</u> WKS data <u>set</u>. Unfortunately, <u>gradient</u> ramp rates and strengths are now approaching values at which neuromuscular stimulation can compromise patient safety and comfort. 2) More stringent assumptions can be made about the <u>image</u> in order to reduce the number of signals necessary to reconstruct it. Some of these "constrained <u>imaging</u>" methods simply apply WKS sampling with stronger assumptions in order to increase the spacing between <u>k-space</u> points (reducing the <u>FOV</u>) or to reduce the <u>k-space</u> sampling limits (reducing <u>image</u> resolution). More novel approaches have utilized prior knowledge to express the <u>image</u> as a superposition of a small number of non-Fourier basis functions. The <u>image's</u> projections onto these basis functions are <u>computed</u> from a reduced <u>set</u> of Fourier <u>encoded</u> signals, or they are measured directly by performing non-Fourier encoding.

Brief Summary Text (7):

In this invention, we take a different approach. We generalize the WKS sampling theorem so that it can be applied to images which are supported on multiple regions within the FOV. By using this "multiple region MR" (mrMR) sampling theorem, such images can be reconstructed from a fraction of the k-space samples required by the WKS theorem. Image reconstruction is performed with FFTs and without any noise amplification, just as in conventional FT MRI. In addition, we show how the method can be applied to a broader class of images having only their high contrast edges confined to known regions of the FOV. If this kind of prior knowledge is available, k-space can be sampled sparsely, and scan time can be reduced. The next section describes the theoretical framework of the mrMR approach. Then, the method is illustrated with simulated data and with experimental data from a phantom. Finally, we describe how the method was used to reduce the time of first-pass Gd-enhanced 3D carotid MRA so that it could be performed without bolus timing.

Brief Summary Text (9):

A method and apparatus are provided for acquiring and reconstructing an image. The method includes the steps of obtaining prior knowledge of the image, possibly by coarse sampling of the image and using the obtained prior knowledge of the image to identify relative locations of structures having relatively high contrast edges. The method further includes the steps of prescribing a set of k-space locations based upon the relative locations of the structures in order to achieve comparable eigenvalues of a reconstruction matrix and sampling the k-space at the prescribed k-space locations to obtain k-space sample data. The k-space sample data are decomposed into background data and edge data. The background data are Fourier transformed to reconstruct a background image component. Similarly, subsets of the edge data are Fourier transformed and the reconstruction matrix is used to form a linear combination of these Fourier transformations in order to reconstruct an edge image component. Finally, the background image component and the edge image component are combined to generate a final image.

Brief Summary Text (10):

Traditional Fourier MR imaging utilizes the Whittaker-Kotel'nikov-Shannon (WKS) sampling theorem. This specifies the spatial frequency components which need be measured to reconstruct an image with a known field of view (FOV) and band-limited spatial-frequency contents. In this paper, we generalize this result in order to find the optimal k-space sampling for images that vanish except in multiple, possibly non-adjacent regions within the \underline{FOV} . This provides the basis for "multiple region MRI" (mrMRI), a method of producing such images from a fraction of the from noise amplification and can be performed rapidly with fast Fourier transforms, just as in conventional FT MRI. The mrMRI method can also be used to reconstruct images that have low spatial-frequency components throughout the entire spatial frequencies (i.e. edges) confined to multiple small regions. The greater efficiency of mrMR sampling can be parlayed into increased temporal or spatial resolution whenever the imaged objects have signal or " edge" intensity confined to multiple small portions of the FOV. Possible areas of application include MR angiography (MRA), interventional MRI, functional MRI, and spectroscopic MRI. The technique is demonstrated by using it to acquire Gd-enhanced first-pass 3D MRA images of the carotid arteries without the use of bolus-timing techniques.

Drawing Description Text (2):

FIG. 1 depicts a schematic outline of an illustrated <u>image</u> reconstruction method in accordance with an embodiment of the invention;

Drawing Description Text (4):

FIG. 3 depicts an image supported on three cells that may be processed using the method of FIG. 1;

Drawing Description Text (5):

FIG. 4 depicts the application of the method of FIG. 1 and FIG. 2 to <u>images</u> of a phantom;

Drawing Description Text (6):

FIG. 5 depicts further details of the application of the method to the phantom images;

Drawing Description Text (7):

FIG. 6 depicts an image of a volunteer processed by the method of FIG. 1 and FIG. 2;

Drawing Description Text (8):

FIG. 7 depicts additional detail of the image of FIG. 6;

Drawing Description Text (10):

FIG. 9 is a block diagram of apparatus that may be used to practice the method of FIG. 1 and FIG. 2.

Detailed Description Text (3):

The mrMRI method of $\overline{\text{an ill}}$ ustrated embodiment of the invention is schematically outlined in FIGS. la-e. In FIG. la, the image to be reconstructed (top panel) vanishes except in three cells that covered the FOV (bottom panel). In FIG. 1b, the composite sampling pattern used to reconstruct the mrMR image from a small number of Fourier components is shown. This pattern is composed of a number of sparse grids, each offset by a different amount from the center of k-space. In this example, the data sampled at all of these points comprise just 1/12 of the WKS data set needed for reconstruction of the entire FOV with the same resolution. In FIG. 1c is shown the "reduced FOV" images, S.sub.a (x,y), which were produced by inverse FT of data on each of the sparse grids in panel b (FIG. 1b). Each of the images is a linear combinations of all the cell \underline{images} , I.sub.j (x,y). Only the magnitudes of these complex \underline{images} are shown. In FIG. 1d, the contents of each cell, found by linearly combining the "reduced FOV" images in panel c is shown. In FIG. 1e, the mrMR created by tiling the FOV with the cell images in panel d is shown. This image is windowed identically to the "exact" image in panel a.

Detailed Description Text (4):

A flow chart of the <u>process</u> depicted in FIGS. 1a-e may be as shown in FIG. 8.

Apparatus 100 that may be used to practice the <u>process</u> shown in FIGS. 1 and 8 may be as shown in FIG. 9. Reference shall be made to these figures as appropriate to understanding the invention.

<u>Detailed Description Text</u> (5):

Consider an arbitrary image in the xy-plane (top panel of FIG. 1a). Cover this plane with an infinite array of rectangular cells with any convenient dimensions (.DELTA.x and .DELTA.y) along the x and y axes, respectively (bottom panel of FIG. 1a). If the image were supported on only one cell, the WKS sampling theorem would dictate that k-space be sampled by the data acquisition device 102 of FIG. 9 on a single coarse grid with spacing equal to .DELTA.k.sub.x =2.pi./.DELTA.x and .DELTA.k.sub.y =2.pi./.DELTA.y along the k.sub.x and k.sub.y axes, respectively. It can be shown that an image supported on C such cells can be reconstructed from sparse data on C (or more) such sparse grids, each grid being offset by a different amount from the center of k-space (FIG. 1b).

<u>Detailed Description Text</u> (6):

First, let I(x,y) be the <u>image</u> to be reconstructed, and denote its Fourier transform by I(k.sub.x,k.sub.y): ##EQUI## where all integrations extend from minus infinity to plus infinity, unless specified otherwise. Define the "comb" sampling function,

III(k), to be ##EQU2## Next, define the function S.sub.a (k.sub.x,k.sub.y) to be ##EQU3## where k.sub.a .ident.(k.sub.ax,k.sub.ay) is the offset between the a.sup.th sampling grid and the origin of k-space; a=1, . . . , A; and A is the number of coarse grids that are superposed to form a composite sparse sampling pattern. Equations (2) and (3) show that S.sub.a (k.sub.x,k.sub.y) simply represents the image's Fourier components on the a.sup.th grid and can be determined experimentally by measuring MR signals that are Fourier -encoded with the appropriate wave vectors. Taking the inverse FT of Eq. (3) produces (FIG. 1c) ##EQU4## Let the integers (m, n) label each cell in the xy-plane with respect to any convenient cell that is labeled (0, 0) and is centered at (x.sub.0, y.sub.0) (FIG. 1a). Let us define I.sub.j (x,y) to be the function produced by translating the contents of the j.sup.th cell, located at cell coordinates (m.sub.j, n.sub.j), to the cell at (0, 0):

Detailed Description Text (10):

and ##EQU8## In other words, each experimentally-determined function S.sub.a (x,y) is a linear combination of all the cell <u>images</u> I.sub.j (x,y). Notice that the contribution of each cell is weighted by a constant complex number, which depends on the offset of the coarse grid from the center of <u>k-space</u> (k.sub.a) and on the locations of the cells (m.sub.j)

Detailed Description Text (11):

Up to this point, no assumptions have been made about the <u>image</u>. Now let us apply a more flexible version of the WKS constraint on the <u>FOV</u>. Assume that only C of the cell <u>images</u> are non-zero; i.e. all of the remaining elements of I are zero. In this case the A.times..infin. matrix M can be replaced by an A.times.C matrix, and the .infin.-dimensional vector I can be replaced with a C-dimensional vector, with j varying over only the non-vanishing cells. If we have measured data on A coarse grids (A.gtoreq.C), we are left with a system of A equations in C unknowns. The C non-vanishing functions I.sub.j can be found by inverting the A linear equations of the form of Eqs. (6) and (7). The solution is ##EQU9## j.epsilon.non-zero cells, (9) or in matrix notation

Detailed Description Text (13):

Notice that we have only imposed a spatial constraint on the $\frac{image's}{s}$ region of support. We have not made any assumptions about the $\frac{image's}{s}$ spatial frequency content within the signal-containing cells. This latter assumption determines the $\frac{k-space}{s}$ limits (and therefore the $\frac{total}{s}$ size) of each of the A sparse grids, and ultimately determines the resolution of the $\frac{image}{s}$ within the cells.

<u>Detailed Description Text</u> (14):

B. Optimal Sampling

Detailed Description Text (15):

Equations (9) and (10) can be used to reconstruct the image from experimental data on A coarse k-space grids with appropriate offsets. Notice that the matrix M depends on the values of these offsets, as well as on the locations of the supporting cells (Eq. (8)). In the absence of noise, any offsets leading to a non-singular M can be used to accurately reconstruct the image, as long as the number of coarse sampling grids is at least as great as the number of non-zero cells in the image (i.e. A.gtoreq.C). However, in the presence of noise, the conditioning of M (or equivalently M.sup.+ M) determines the amount of noise amplification during reconstruction. Specifically, noise in the experimental data will be amplified during the reconstruction process to the extent that M is ill-conditioned (i.e. to the extent that some of the eigenvalues of M.sup.+ M are much smaller than others). Therefore, one expects that image noise will be minimized if the k-space offsets are chosen so that these eigenvalues are all equal.

Detailed Description Text (16):

To prove this, we use Eqs. (9) and (10) to calculate the mean squared noise propagating from the experimental data into the reconstructed image I(x,y). Assume that the root-mean-squared noise in I(k.sub.x,k.sub.y) is .epsilon. and that there is no correlation between the noise at different k-space locations. Then, it follows from Eqs. (9) and (10) that the mean squared noise in the image is: ##EQU10## where the brackets denote the statistical average, the integral extends over the C cells that support I, and each coarse k-space grid has the dimensions N.sub.x

.times.N.sub.y. The trace on the right side is equal to ##EQU11## where .mu..sub.i denotes the i.sup.th eigenvalue of the C.times.C Hermitian matrix M.sup.+ M. Notice that Eq. (8) implies that these eigenvalues must lie on a hyperplane in .mu.-space defined by ##EQU12## Straight-forward application of multivariable calculus shows that the trace in Eq. (12) has a global minimum on this hyperplane when all .mu..sub.i =A (i=1, . . . , C). Therefore, as we expected, the level of noise in an mrMR image is minimized when the A coarse sampling pattern offsets are chosen such that these eigenvalues are all equal. Notice that for this optimal sampling pattern, ##EQU13## where NEX.ident.A/C is the ratio of the number of acquired k-space points to the minimal number.

Detailed Description Text (17):

Notice that the eigenvalues of M.sup.+ M are equal to one another if and only if this matrix is equal to A times a C.times.C identity matrix. Using the definition of M (Eq. (8)), M.sup.+ M has this form if and only if ##EQU14## for all unequal j and j', where d.sub.jj, is the displacement vector between the centers of any two supporting cells, located at (m.sub.j, n.sub.j.) and (m.sub.j, n.sub.j.). Equation (14) shows explicitly how the optimal offsets of the sampling pattern (k.sub.a) are determined by our prior knowledge of the locations of the supporting cells (d.sub.jj'). Notice that Eq. (14) only depends on the relative locations of the supporting cells. Therefore, the optimal sampling pattern is not changed if the cell array is translated across the FOV in order to most efficiently contain the intensity distribution of a particular image.

Detailed Description Text (18):

To summarize, we have shown that the offsets of the A coarse k-space grids should be chosen so that Eq. (14) is satisfied for all pairs of supporting cells. If this can be achieved, <u>image</u> reconstruction (Eqs. (9) and (10)) will be perfectly well-conditioned, and image noise will be minimized. In fact, the level of noise will be the same as in a conventional (WKS sampled) FT image having the same resolution over an equal area of support (i.e. over a rectangular FOV with area equal to C.DELTA.x .DELTA.y). This last statement is a consequence of the following two facts: 1) the level of noise in an mrMR image does not depend on the positions of the supporting cells; 2) if the supporting cells are rearranged into a rectangular array (e.g. into a single row of adjacent cells), the WKS sampling pattern is an optimal (mrMR) sampling pattern. The first fact follows immediately from Eq. (11) and the fact that Tr[(M.sup.+ M).sup.-1] is independent of the supporting cells' positions; namely, for an optimal sampling pattern, it is equal to C/A or 1/NEX. To understand the second statement, <u>imagine</u> that the supporting cells form an N.sub.x .times.N.sub.y rectangular array. The WKS sampling pattern for this "reduced FOV" can be broken down into a composite of A=N.sub.x N.sub.y coarse k-space grids, having the offsets: ##EQU15## where p.sub.a =0, 1, . . . , N.sub.x -1 and q.sub.a =0, 1, . . . , N.sub.y -1. For these offsets, the mrMR matrix element M.sub.aj in Eq. (8) is e.sup.-2.pi.ip.sbsp.a.sup.m.sbsp.j.sup./N.sbsp.x e.sup.-2.pi.iq.sbsp.a.sup.n.sbsp.j.sup./N.sbsp.y. Each of these factors is a component of a discrete Fourier function. It follows from their completeness and orthogonality that M.sup.+ M=N.sub.x N.sub.y I=A I, where I is the identity matrix. Therefore, the WKS sampling pattern leads to an M.sup.+ M matrix having all eigenvalues equal to A, proving the assertion that it is also an optimal mrMR sampling pattern. Therefore, we have proved that the noise level in an mrMR the same as that for a WKS image of a rectangular region formed by the rearrangement of the supporting cells.

<u>Detailed Description Text</u> (20):

We now show how the system 100 may use a variant of mrMRI to reconstruct an image that has non-zero intensity throughout the entire FOV but has high contrast edges confined to multiple regions within the FOV. Suitable filters can be used to decompose such an image into the sum of a slowly undulating "background" component and an "edge" component that is only supported on small portions of the FOV. The former component can be reconstructed from data in a small "keyhole" at the center of k-space, and the latter component can be reconstructed from sparse k-space data in an optimal mrMR sampling pattern. FIG. 2 outlines this filtered mrMRI technique.

Detailed Description Text (21):

FIG. 2a, shows the image to be reconstructed (left panel) consisted of a slowly

undulating background component, superposed on an edge component that was supported on only three cells (right panel). FIG. 2b, shows the k-space representation of the Hamming filter which may be used to decompose the image into background and edge components. FIG. 2c. shows the background component (right panel) and its FT (left panel), which may be used to define the product of the FT of the exact image (panel a) and the Hamming filter (panel b). FIG. 2d shows the edge component (right panel) and its FT (left panel), which may be used to define the product of the FT of the exact image (panel a) and the complement of the Hamming filter (panel b). FIG. 2e shows the background component (right panel) that may be reconstructed by densely sampling the center of the image's k-space using a keyhole sampling pattern (left panel), applying the low-pass filter (panel b) to these data, and taking the inverse edge component (right panel) that may be FT of this filtered data. FIG. 2f shows the reconstructed by sampling the image's k-space on each of the sparse grids forming an mrMR sampling pattern (left panel), applying the complementary high-pass filter to these data, and then applying the mrMR technique (FIG. 1). FIG. 2g shows the mrMR image, created by adding the reconstructions of the background and edge components (panels e and f). This image was reconstructed from just 1/9 of the WKS k-space data required to create an image of the entire FOV with the same resolution. This image is windowed identically to the exact image in panel a. FIG. 2h shows the error formed by taking the magnitude of the difference between the mrMR image (panel q) and the exact (WKS) image (panel a). This image has been windowed to accentuate the faint discrepancies.

Detailed Description Text (22):

First, note that the FT of any <u>image</u> can be decomposed into complementary components (FIGS. 2c and 2d) that are low-pass filtered and high-pass filtered, respectively:

Detailed Description Text (23):

where I(k.sub.x,k.sub.y) is the FT of the image and F(k.sub.x,k.sub.y) is the low-pass filter (FIG. 2b). If F(k.sub.x, k.sub.y) is chosen wisely, B(x,y) will resemble I(x,y) except in the vicinity of high contrast edges which will be modified by blurring and truncation artifact (FIG. 2c), and E(x,y) will vanish everywhere except in the vicinity of the edges of I(x,y) (FIG. 2d). By definition, the background component, B(x,y), can be reconstructed from data in a k-space "keyhole" that is bounded by the cut-off of F(k.sub.x,k.sub.y) (FIG. 2e). Specifically, data can be acquired on the dense WKS grid in this region, multiplied by F(k.sub.x,k.sub.y) and then subjected to an FFT. The result is B(x,y), which comprises a low resolution version of the filtered image. The mrMR method can be used to reconstruct the edge component, E(x,y), from E(k.sub.x,k.sub.y) measured at optimal sparse k-space locations (FIG. 2f). The required values of E(k.sub.x,k.sub.y) can be determined experimentally by measuring the corresponding components of I(k.sub.x,k.sub.y) and multiplying them by the high pass filter 1-F(k.sub.x,k.sub.y). Finally, the \underline{image} I(x,y) is found by summing the reconstructed background and edge components: I(x,y)=B(x,y)+E(x,y), as shown in FIG.

<u>Detailed Description Text</u> (24):

Neither B(x,y) nor E(x,y) will be degraded by noise amplification because both are reconstructed from optimal k-space sampling patterns, determined by the WKS and mrMR sampling theorems, respectively. E(x,y) could be degraded by aliasing if the cut-off frequency of F(k.sub.x, k.sub.y) is too low, causing ringing and blurring patterns in E(x,y) to extend so far from the edges in I(x,y) that they reach beyond the boundaries of the cells used in the mrMR reconstruction. However, this problem can be ameliorated by: 1) using a suitably high cut-off frequency in F(k.sub.x,k.sub.y); 2) designing the shape of F(k.sub.x, k.sub.y) so that the truncation artifact is largely confined to the vicinity of the edges (e.g. a Hamming filter); 3) using cells that are sufficiently large to contain most of the remaining truncation artifact in E(x,y).

<u>Detailed Description Text</u> (25):

In the special case of an <u>image with edges</u> confined to a single region, the filtered mrMR method may be similar to that of certain prior art techniques. Such <u>images</u> may be reconstructed from <u>k-space</u> samples on a single sparse WKS grid, superposed on a pattern of dense sampling in the center of <u>k-space</u>. However, the prior art techniques used a <u>step-like</u> function for F(k.sub.x, k.sub.y). This choice of filter

was suboptimal because F(x,y) in this case was a sinc function, and $\underline{\text{edges}}$ in I(x,y) produced non-localized ringing in E(x,y). This tended to increase the region of

Detailed Description Text (27):

support of E(x,y) and reduced the efficiency of the method.

Suppose that an <u>image</u> is known to be supported on only three cells (FIG. 3) and that the <u>image</u> is to be reconstructed from data on three coarse grids. FIG. 3 shows <u>image</u> that is supported on only three cells, which are separated from each other by displacement vectors d.sub.ij. In this case, Eq. (14) is equivalent to the following three conditions:

Detailed Description Text (29):

First, consider the special case in which the three cells happen to coalesce into a single rectangular region parallel to the x -axis. Then, we have d.sub.12 =d.sub.23 =(.DELTA.x, 0) and d.sub.31 =(-2.DELTA.x, 0), and algebra shows that all solutions to Eq. (16) must satisfy: k.sub.1x -k.sub.3x =1/3.DELTA.k.sub.x and k.sub.2x -k.sub.3x =2/3.DELTA.k.sub.x. The three superposed coarse grids with these offsets comprise the usual WKS sampling pattern for a single region with dimensions 3.DELTA.x.times..DELTA.y. In other words, the general condition for optimal mrMR sampling (Eq. (16)) reduces to the usual sampling theorem in the special case when the three cells coalesce into a single rectangular region. This illustrates the general statement which was proven at the end of IIB: WKS sampling patterns belong to the larger set of optimal mrMR sampling patterns.

Detailed Description Text (30):

Now, suppose that the three cells are at non-collinear locations (FIG. 3). With the help of the fact that d.sub.12 +d.sub.23 +d.sub.31 =0, it can be shown that the only solutions of Eq. (16) are: ##EQU16## where n.sub.i (i=1, . . . , 4) are any integers and D is the matrix: ##EQU17## For example, consider the image in FIG. 1a, which is supported on only three cells of a 6.times.6 cell array. In this case, d.sub.12 = (4.DELTA.x,0) and d.sub.23 = (0,4.DELTA.y), and the solutions in Eq. (17) are k.sub.1 -k.sub.3 = (1/3.DELTA.k.sub.x,5/6.DELTA.k.sub.y) and k.sub.2 -k.sub.3 = (1/6.DELTA.k.sub.x,2/3.DELTA.k.sub.y) when we choose n.sub.1 =1, n.sub.2 =3, n.sub.3 =-1, and n.sub.4 =-3. FIG. 1b shows the optimal composite sampling pattern, created by superposing these three coarse grids and taking k.sub.3 =0 for convenience. Other optimal sampling patterns can be created by substituting different values for n.sub.i. For example, the choices of n.sub.1 =n.sub.2 =1 and n.sub.3 =n.sub.4 =-3 give k.sub.1 -k.sub.3 = (1/3.DELTA.k.sub.x, 1/3.DELTA.k.sub.y) and k.sub.2 -k.sub.3 = (2/3.DELTA.k.sub.x, 2/3.DELTA.k.sub.y)

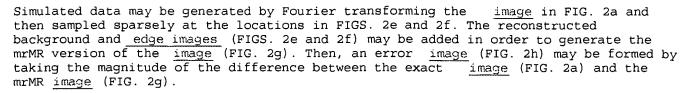
Detailed Description Text (31):

The mrMR method may be tested by using it to reconstruct the 192.times.192 image in FIG. 1a from simulated data in an optimal mrMR sampling pattern. Simulated data may be generated by Fourier transformation of the image in FIG. 1a and then sampled sparsely according to the sampling pattern in FIG. 1b. The number of sampled data was 1/12 of the data needed for a conventional FT reconstruction of the entire FOV with the same resolution. These simulated data may be substituted into the right side of Eq. (9) or (10) in order to reconstruct the mrMR version of the image (FIG. 1e).

Detailed Description Text (32):

The filtered mrMR method may be tested by using it to reconstruct the 192.times.192 image in FIG. 2a from simulated data. The filter, F(k.sub.x, k.sub.y), may be chosen to be a Hamming filter that was cut off along the edges of a 32.times.32 square in the center of k-space (FIG. 2b). The effect of this filter is shown in FIGS. 2c and 2d, which depict the background and edge components of the image in FIG. 2a. By definition, the background component is band-limited to a 32.times.32 region of k-space. Therefore, it can be reconstructed exactly from a 32.times.32 array of data on the WKS grid (FIG. 2e). Notice that the intensity in the edge image in FIG. 2d is confined to the same three cells that support FIG. 1a. Therefore, this edge image should be accurately reconstructed from the sparse mrMR sampling patterns derived for FIG. 1a (namely, the sampling pattern in FIG. 1b or FIG. 2f). The composite sampling pattern may be created by combining the "keyhole" of data required to reconstruct the background component (FIG. 2e) with the edge component sampling scheme (FIG. 2f). These combined data comprised only 1/9 of the complete WKS set.

7 of 20 10/27/2003 9:01 AM



Detailed Description Text (34):

To demonstrate the validity of the technique described above, the mrMRI technique was used to image a carotid artery phantom (FIGS. 4 and 5) consisting of two branching plastic tubes having an inner diameter equal to 5 mm. FIG. 4a shows a low resolution "scout" image of the carotid artery phantom, with a superposed 4.times.8 array of rectangular cells. FIG. 4b shows the same scout image after the cell array was translated and "sheared" in the y -direction so that all the vessels fell within just two cells. Note that translation and shearing of the cell array (possibly on a slice-by slice basis) does not change the optimal sampling pattern dictated by mrMR.

Detailed Description Text (35):

FIG. 5a shows the "exact" image of a typical axial slice of the phantom, generated by FT of 16,384 (128.times.128) phase <u>-encoded</u> signals. FIG. 5b shows the <u>k-space</u> locations of Fourier components that are optimal for mrMR reconstruction of all slices in the phantom. These comprise less than 1/8 of the WKS data set used to produce the exact image in panel a. FIG. 5c shows the mrMR image of the axial slice in panel a, reconstructed from the signals at the k-space locations in panel b. This image is windowed identically to panel a. FIG. 5d shows the "error" image produced by subtracting the exact image in panel a from the mrMR reconstruction in panel c and windowing the result to increase the conspicuity of the faint discrepancies. FIG. 5e shows MIPs created from all of the exact axial images. FIG. 5f shows MIPs created from the mrMR reconstructions. This image is windowed identically to panel e. FIG. 5g shows an image of the errors in the mrMR MIPs, produced by subtracting the exact MIPs in panel e from the mrMR MIPs in panel f and windowing the result to accentuate the faint discrepancies.

Detailed Description Text (36):

The tubes were filled with a concentrated gadolinium solution (gadodiamide (Omniscan), Nycomed, Inc., Wayne, Pa.) and were immersed in a bath of very dilute gadolinium solution. The phantom was placed in the quadrature bird-cage head coil of a 1.5 T whole body scanner (Signa, General Electric Medical Systems, Milwaukee, Wis.). A 3D spoiled gradient echo pulse sequence (17) was used with TR=4.1 ms, TE=1.6 ms, flip angle=20.degree. This pulse sequence selectively excited a coronal slab that had RL.times.AP.times.SI dimensions of 160.times.160.times.160 and contained the "arteries". The slab was phase encoded in the transverse plane and frequency encoded along the SI direction to produce a 128.times.128.times.128 data array, resulting in an isotropic 1.25 mm resolution. These 16,384 k-space signals were obtained in 67 seconds.

Detailed Description Text (37):

Next, a small <u>subset</u> of these signals was used to reconstruct mrMR <u>images</u> of ear axial section. The filtered mrMR technique was applied in order to account for the images of each bath's signal intensity, which varied slowly across the entire FOV. The background component of each image was defined by Eq. (15), with F(k.sub.x,k.sub.y) equal to a Hamming filter with a cut-off at the $\underline{\text{edges}}$ of a 32.times.32 square in the center of k-space. This background image was reconstructed by conventional FFTI of the signals that densely sampled this region, after they had been multiplied by the Hamming filter. The complementary $\underline{\text{edge image}}$ was expected to vanish except in the vicinity of the vessels, and was reconstructed from $\underline{\text{k-space}}$ samples in the sparse mrMR pattern dictated by the locations of the vessel-containing cells. In an actual clinical situation, a scout scan of the neck would have been used to ascertain the relative positions of the vessels, as demonstrated in the next section. In the case of the phantom, the vessels were located on low resolution (32.times.32) axial sections of the above-described coronal <u>slab</u>. The <u>FOV</u> of these axial sections was covered by a 4.times.8 array of rectangular cells (FIG. 4a) with dimensions: .DELTA.x=40 mm and .DELTA.y=20 mm. This array was translated and sheared so that the vessels were contained in just two cells (i.e. C=2), which were separated by one

8 of 20

empty cell along the x -direction (FIGS. 4a and 4b). As shown below, the contents of the sheared cells can be reconstructed without noise amplification from the mrMR sampling pattern for unsheared cells. An mrMR edge image for each axial section was reconstructed from a sparse subset of the acquired signals, which included the k-space points on two coarse grids, i.e. A=2. The mrMR sampling criterion in Eq. (14) dictates that the offsets of these grids (k.sub.1 and k.sub.2 k) satisfy:

 $\frac{\text{Detailed Description Text}}{\text{where J is an odd integer.}} \quad \text{(39):}$ unsheared \underline{edge} -containing cells was d=(2.DELTA.x, 0), Eq. (19) implies that k.sub.1x $-k.sub.2x = \overline{J/4}.DELTA.k.sub.x$, where .DELTA.k.sub.x = 2.pi./.DELTA.x and J is any odd integer. This constraint was satisfied with J=1, k.sub.1 = (1/4.DELTA.k.sub.x, 0), and k.sub.2 =0, which corresponds to the two coarse grids in FIG. 5b.

Detailed Description Text (40):

Parenthetically, it is interesting to notice what would have happened if the cells had been adjacent (d=(.DELTA.x,0)). In that case, Eq. (19) would have dictated that k.sub.1x - k.sub.2x = J/2.DELTA.k.sub.x, where J is again an odd integer. For all values of J, this implies that the two coarse grids must be offset by 1/2.DELTA.k.sub.x with respect to one another, thereby forming the usual WKS sampling pattern for a single rectangular region with dimensions 2.DELTA.x.times..DELTA.y. This example is another illustration of the fact which was proven in general at the end of IIB: the optimal mrMR sampling patterns include to the usual WKS sampling when the cells coalesce into a single rectangular region.

Detailed Description Text (41):

In order to reconstruct the edge component of the image, the data on each of the 32.times.16 coarse grids was multiplied by the complement of the Hamming filter, and each of these filtered data sets was inverse Fourier transformed. The resulting functions S.sub.a (x,y) were used to compute images of the two sheared edge-containing cells with 1.25 mm.times.1.25 mm resolution. The resulting image was added to the previously-described background image to create the mrMR image (FIG. 5c). This should be compared to the exact image (FIG. 5a), which was reconstructed by FT of the 16,384 data in the complete (128.times.128) WKS sampling pattern. Notice that the mrMR image was reconstructed from the 1,984 data in the composite sampling pattern (FIG. 5b), which comprised less than 1/8 of the complete data set. FIG. 5d shows the error image that was equal to the magnitude of the difference between the exact image (FIG. 5a) and the mrMR image (FIG. 5c). Finally, maximum intensity projection (MIP) images were created from the exact and mrMR reconstructions (FIGS. 5e and f), and differences between these MIPs were displayed in corresponding error images (FIG. 5g).

Detailed Description Text (42):

As mentioned above, for some axial images, the cell array had to be sheared along the y-axis so that the vessels were contained in just two cells (FIG. 4b). However, it is easy to see that the contents of the sheared cells can still be reconstructed from the mrMR sampling pattern derived for the unsheared cells. In fact, this can be done whenever each non-zero cell occupies a different cell column and the k.sub.a offsets all lie on the k.sub.x axis. In this situation, the sparse sample spacing in the k.sub.y direction is determined only by the y-extent of the image intensity in each pixel column, independent of the cell width. Therefore, the 2D mrMR reconstruction is equivalent to a 1D mrMR reconstruction in the x-dimension and a conventional 1D "reduced FOV" reconstruction in the y-dimension. As long as the image intensity in each column does not extend over a segment greater than the height of a single cell (.DELTA.y), it can be positioned in a continuous manner anywhere within that particular column, and the resulting cell array will appear to be sheared in the y-dimension. The additional flexibility of this shearing strategy allows one to customize the cell shapes on a slice by slice basis without affecting the optimal mrMR sampling pattern. This reduces both the height of the cells needed to contain the image's edges and the number of k-space points needed to successfully reconstruct the image. It should be noted that this shearing method can also be applied to certain arrangements of supporting cells in which some cell columns contain more than one supporting cell; however, such cases were not encountered in the experiments described here.

Detailed <u>Description Text</u> (44):

The mrMR method was used to perform first-pass Gd-enhanced 3D MRA of the carotid arteries of a patient volunteer. Informed consent was obtained from the patient, a 68 year-old male who was scheduled to undergo an infused brain MRI. After the uninfused portion of the brain exam was completed, the patient underwent an unenhanced 2D TOF neck MRA with the same neurovascular coil used for the brain study. These images were obtained for comparison to the subsequent Gd-enhanced mrMRA images. 2D TOF was performed with a spoiled gradient echo pulse sequence with TR=23 ms, TE=4.9 ms, flip angle=60.degree., first order flow compensation, and fractional echo. Each axial section was 1.5 mm thick and was imaged with a 256.times.224 matrix across a 180 mm.times.180 mm FOV. Thus, the overall spatial resolution was 0.7 mm.times.0.8 mm.times.1.5 mm along the RL.times.AP.times.SI directions, respectively. It took 5 seconds to acquire a 2D TOF image of each axial section.

Detailed Description Text (45):

The k-space sampling pattern for the Gd-enhanced mrMRA was planned in an on-line fashion with the help of a scout image of the patient's anatomy. The scout the axial MIP ("collapsed" image) of a 2D TOF MRA study of 10 thick axial sections covering the carotid bifurcation. It took 50 seconds to acquire these images with high resolution (256.times.192) in the transverse plane. However, an adequate scout could easily have been obtained in much less time by increasing slice thickness and decreasing resolution. The scout image was used to create a cell array which could be translated and sheared so that the arteries were contained in just two cells, separated by a single "empty" cell. FIG. 6a shows the resulting cells, which had dimensions equal to 24 mm.times.30 mm and belonged to an 8.times.4 array that covered a 190 mm.times.120 mm region of the FOV. FIG. 6a is an axial "scout" of the neck of a patient volunteer with a superposed array of cells, just two of which contained the carotid and vertebral arteries. FIG. 6b is the sparse pattern of 862 k-space locations that are optimal for reconstructing an image with edges confined to the two vessel-containing cells in panel a. FIG. 6c is a typical Gd-enhanced axial image reconstructed from data at the sparse k-space locations in panel b. This is the average of two mrMR images, produced from the two 3D mrMRA scans that coincided with the first arterial pass of the contrast agent. FIG. 6d are complete set of mrMRA images MIP views of the carotid bifurcations, created from the like the one in panel c.

Detailed Description Text (46):

FIG. 6e is the corresponding MIPs, reconstructed from unenhanced 2D TOF MRA images. Note the loss of TOF flow signal in both carotid bulbs (arrows) which is not observed in the Gd-enhanced MIPs.

Detailed Description Text (47):

The relative positions and dimensions of the cells of FIG. 6a were used to prescribe the k-space sampling pattern to be used in the subsequent Gd-enhanced mrMRA pulse sequence. Because the edge component of the image was expected to vanish (or nearly vanish) except in the two artery-containing cells, Eqs. (9) and (10) could be used to reconstruct it from data on two coarse grids. As in the phantom study, the displacement vector between the centers of the two unsheared supporting cells was d=(2 .DELTA.x, 0). Therefore, the mrMR sampling theorem dictated that the two coarse grids be superposed with the optimal offsets (Eq. (19)): k.sub.1 = (1/4).DELTA.k.sub.x, 0) and k.sub.2 = 0, where .DELTA.k.sub.x = 2.pi./.DELTA.x. The dimensions of these grids were chosen to be 20.times.16, so that the edge image would have spatial resolution equal to 1.2 mm.times.1.9 mm. The image's background component was reconstructed from the data on a dense 24.times.10 grid at the center of k-space, after multiplying those data by a Hamming filter covering that region. FIG. 6b shows the composite mrMR sampling pattern, which was comprised of the two large coarse grids, together with the small dense grid. This sampling pattern contained just 862 of the 10,240 WKS measurements required to achieve uniform 1.2 mm.times.1.9 mm resolution throughout the entire

<u>Detailed Description Text</u> (48):

The patient was infused with 0.3 mM/kg of gadodiamide contrast agent (Omniscan, Nycomed, Wayne, Pa.) over a 25 second time period. The mrMRA scan was performed repetitively before, during, and after the injection, using a 3D spoiled gradient echo pulse sequence (17) with TR=8 ms, TE=1.7 ms, and flip angle=45.degree. A 120

mm thick coronal <u>slab</u> was selectively excited. It was frequency <u>-encoded</u> along the SI <u>direction</u> in order to produce 1.2 mm thick axial sections. The signals were <u>phase-encoded</u> along the x (RL) and y (AP) <u>axes</u> according to the composite sampling pattern shown in FIG. 6b. It took just seven seconds to acquire the 862 <u>phase-encoded</u> signals in this pattern. The mrMRA pulse sequence was run seven times in quick succession over a 49 second time period that began seven seconds before the infusion and ended seventeen seconds after the <u>completion</u> of the infusion. In this way, acquisition of a <u>complete</u> mrMR data <u>set</u> was ensured during the first arterial pass of contrast agent without the need for "hit or miss" bolus timing techniques.

Detailed Description Text (49):

The signals from non-vascular tissues were suppressed by subtracting the pre-infusion mrMRA data from each subsequent data set. In order to identify the arterial phase, low resolution images were reconstructed from each subtracted mrMRA data set by 2D FT of the signals in the center of k-space. As shown in FIG. 7, these images clearly demonstrate early arterial enhancement, followed by venous enhancement.

Detailed Description Text (50):

FIG. 7 shows low resolution axial <u>images</u> of the neck of the patient volunteer in FIG. 6, at six time intervals after the Gd infusion. These <u>images</u> were produced by 2D FT of the signals acquired in the center of <u>k-space</u> during each of the last six Gd-enhanced mrMRA <u>scans</u>, after the corresponding signals from the first <u>scan</u> were subtracted in order to suppress the intensity of stationary tissues.

Detailed Description Text (51):

In order to maximize contrast-to-noise, the subtracted data from the fourth and fifth \underline{scans} was averaged, both of which showed arterial enhancement without significant venous signal. The subtracted data in the densely sampled square at the center of \underline{k} -space were multiplied by the Hanmming filter that covered that area, and the background component of the mrMR \underline{image} was reconstructed by FFT of this filtered data. The \underline{edge} component of the mrMR \underline{image} was reconstructed from the subtracted data on the two coarse \underline{k} -space grids, after the data had been multiplied by the complement of the Hamming filter (see Eq. (15)) and Fourier transformed. The $\underline{complete}$ mrMR \underline{image} was calculated by adding the resulting \underline{edge} component to the background component (FIG. 6c). Finally, MIPs of the mrMRA reconstructions were created and compared to MIPs of the unenhanced 2D TOF \underline{images} acquired prior to infusion (FIGS. 6d and e).

Detailed Description Text (54):

FIG. 1e shows the mrMR reconstruction of the simulated image in FIG. 1a. The two images are identical to within round-off error, despite the fact that the former image was reconstructed from 1/12 of the data used to reconstruct the latter one. FIG. 2g shows the mrMR reconstruction of the simulated image in FIG. 2a. Notice the accuracy of the result, even though it was reconstructed from sparse data (FIGS. 2e and 2f) which comprised only 1/9 of the complete FT data set. FIG. 2h is the error image, which is the magnitude of the difference between the mrMR image and the exact image. This image is windowed to show the discrepancies. These errors were caused by some low spatial frequencies in the edge component which were outside the three supporting cells and led to <u>aliasing when this edge image</u> was reconstructed by mrMR. Notice that this error is comprised solely of low frequency image components; i.e. the image's edges are reconstructed faithfully.

Detailed Description Text (56):

FIG. 5a shows the exact image of a typical slice at the level of the tubing bifurcations, reconstructed from the complete set of 16,384 data required to image the entire FOV with an isotropic 1.25 mm resolution. FIG. 5c shows the mrMR image that was created from sparse data at the k-space locations in FIG. 5b, which comprised less than 1/8 of the complete FT data set. FIG. 5d is the error image, equal to the magnitude of the difference between the mrMR image and the exact image. This image is windowed to increase the conspicuity of the faint aliasing artifacts. The error image also shows truncation artifacts at the surface of the bath, which was outside the two edge-containing cells. FIGS. 5e and 5f show maximum intensity projections (MIPs) created from the exact and mrMR reconstructions, respectively. Notice that the mrMR MIP accurately depicts the tiny "step-off" discontinuities of

the lumen where the caliber of the tubing changes abruptly. These features resemble minimal atherosclerotic plaques. Only faint $\frac{\text{artifacts}}{\text{are present}}$, as demonstrated by the MIP error $\frac{\text{image}}{\text{discrepancies}}$ (FIG. 5g), which is windowed to accentuate these discrepancies.

Detailed Description Text (58):

FIG. 6c shows a typical axial mrMR $\frac{image}{image}$ that was reconstructed from the data at the 862 k-space locations in FIG. 6b. FIG. 6d shows MIP $\frac{images}{images}$ derived from mrMR $\frac{images}{images}$ of 60 such axial sections. These should be compared to the MIPs of the unenhanced $\frac{images}{images}$ in FIG. 6e. Notice that the 2D TOF MIPs are degraded by signal loss in the carotid bulbs, which are the most common locations of atherosclerotic plaques. In contrast, the mrMRA MIPs depict the full extent of the carotid bulbs.

Detailed Description Text (60):

If the FT of a signal is limited to a single band, the WKS sampling theorem shows how to collect the minimum number of samples from which the entire signal can be reconstructed without noise amplification. Conventional FT MRI is based on this theorem. A more general sampling theorem is described below which shows how to sample the k-space of an image that vanishes except in multiple regions (i.e. it is "multi-banded" in image space). These data can be used to reconstruct the image without noise amplification; i.e. the image has the same noise level as a comparable conventional FT image with the same spatial resolution over the same total area of support. Furthermore, it is demonstrated below that this method can be modified to handle a larger class of images: those that have slowly varying signal intensity across the entire FOV and high-contrast edges confined to small regions. The "background" component of such an image can be reconstructed from densely sampled data in the center of k-space, while its "edge" component can be reconstructed from the sparse k-space samples dictated by the new sampling theorem.

Detailed Description Text (61):

If the edge-containing regions cover only a small portion of the FOV, the image can be reconstructed without noise amplification from a sparse subset of the complete (WKS) data set. This makes it possible to use prior knowledge of the object to increase the efficiency of the sampling process. This can be advantageous in several ways. In many cases, mrMR images can be acquired in less time (or with greater spatial resolution) because it takes fewer TR intervals to sample the image at the sparse mrMR k-space locations than at the more numerous WKS points. Furthermore, if k-space trajectories are used to collect multiple k-space samples per TR interval, lower bandwidth and/or shorter read-out time (trajectory traversal time) can be used because it is only necessary to visit the sparse k-space locations needed by mrMRI. Reducing the bandwidth leads to increased signal-to-noise, while shortening the read-out time tends to reduce artifacts due to off-resonance effects.

Detailed Description Text (62):

It should be noted that the mrMR method is computationally cheap, because <u>images</u> are formed from linear combinations of small FFTs of the data. For <u>imaging</u> situations in which the supporting cells occupy only a small fraction of the entire <u>FOV</u>, the reconstruction process is computationally cheaper than that of conventional FT MRI, because the latter involves a single large FFF. In the experiments discussed here, a single R10000 processor 104 (Silicon Graphics, Inc., Mountain View, Calif.) <u>computed</u> each mrMR <u>image</u> in a small fraction of a second. In fact, in the current implementation, the speed of mrMR <u>image</u> reconstruction was limited by extraneous factors, such as the time required for the Unix script to call the reconstruction routine and the time required to print a message on the user's screen.

Detailed Description Text (63):

The mrMR method was applied to simulated data and to experimental data from a vascular phantom. When the resulting images were compared to "exact" images, it was apparent that there was no noise amplification and that little aliasing or truncation artifact was produced by the presence of a slowly undulating background intensity. It was also shown how mrMRI could be used to perform first-pass Gd-enhanced 3D carotid MRA in just 7 seconds. The exam was performed in a fashion analogous to conventional angiography: namely, a series of 3D mrMRA scans was performed before, during, and after the injection of contrast agent. The resulting data were used to retrospectively identify the first arterial pass of contrast. In

other words, it was not necessary to "catch" the arterial phase with bolus timing procedures, which can be operator-dependent and patient-dependent (13-16). Bolus timing can be particularly ticklish for Gd-enhanced carotid <u>imaging</u> because the internal jugular veins enhance within 10 seconds of the first arterial pass of contrast agent and because they are immediately adjacent to the carotid arteries.

Detailed Description Text (64):

The mrMRI method may also be useful in other <u>imaging</u> situations in which the high spatial frequencies are known to be confined to multiple regions of the <u>FOV</u>. For example, this type of prior knowledge may be available in functional MRI, interventional MRI, and MR spectroscopic <u>imaging</u>, as well as in other applications of MRA. Three-dimensional MR spectroscopic <u>imaging</u> may benefit from extensions of mrMRI to higher dimensions. Moreover, the new sampling theorems might increase the sampling efficiency of other Fourier <u>imaging</u> modalities, such as radio astronomy, radar, and crystallography. It may also be applied in telecommunications for the purpose of digitizing and reconstructing signals with frequency components in multiple frequency bands.

Detailed Description Text (65):

There are two principle sources of image degradation in mrMRI reconstructions. First of all, the SNR of mrMR images is limited by the total number of measured signals, just as in conventional FT reconstruction. The SNR of our carotid mrMRA suboptimal because they were reconstructed from just 862 k-space samples and because no attempt was made to optimize our pulse sequence and infusion protocol. Secondly, any high spatial frequency features (i.e. edges) which fall outside of our specified cells (thereby violating our assumptions) will alias into these cells. These artifacts can be minimized by using techniques that increase the contrast of within the specified cells and simultaneously suppress the contrast of edges outside of these cells. Image quality may also be improved by: 1) optimization of the contrast-to-noise of the pulse sequence (e.g. use of fat suppression, fractional echoes, and more suitable values of the TR, bandwidth, and flip angle parameters); 2) utilization of a power injector in order to increase the concentration of gadodiamide in the blood; 3) use of better spatial filters for separating the into background and edge components; 4) creation of the mrMRA images from temporally-filtered signals collected during all seven mrMR scans (not just during one or two arterial acquisitions as in IIIC). By making use of data from all of the mrMRA acquisitions, significantly higher SNR may be achieved (e.g., 2-3 times higher). Similar temporal filtering methods have been developed for conventional X-ray angiography.

Detailed Description Text (67):

It is instructive to compare mrMRI to Locally Focused MRI (LF MRI), also developed by the inventors. In most situations, the mrMR method is preferable because it avoids the noise amplification of LF MRI and because it is computationally much cheaper than LF MRI. In order to perform LF MRI, the first step is to generate a set of non-Fourier basis functions that span the space of all images having the pattern of spatial variation suggested by prior knowledge. The Fourier components of the image are linearly related to the image's projections onto these LF basis functions. Therefore, these linear equations can be inverted to calculate the basis function coefficients in terms of an equal number of measured Fourier components. If our prior knowledge is strong enough to be expressed by a small number of basis functions, the image can be reconstructed from a small number of k-space samples. Notice that the LF MRI method is quite general, allowing the user to exploit prior knowledge of the image's general pattern of spatial variation in multiple regions of irregular shape. The main problem is that LF images are degraded by noise amplification, caused by ill-conditioning of the matrix inversion required to find the basis function coefficients. The elements of this matrix depend on the sampling pattern, as well as on the form of the basis functions dictated by our prior knowledge. In general, it has not been possible to find minimal sampling patterns that make this matrix well-conditioned (i.e. that make its singular values approximately equal). In order to make the problem better conditioned, it has been necessary to over-determine its solution by sampling 4-6 times more k-space points than the number of basis functions. Of course, this is undesirable because it increases scan time by a factor of 4-6 above the minimal LF MRI requirements. The second disadvantage of the LF technique is its computational

13 of 20 10/27/2003 9:01 AM

expense. Image reconstruction requires the inversion of a matrix that has dimensions equal to the number of basis functions, which is itself proportional to the total area of the edge-containing regions. For example, a 400 times 400 matrix was inverted in order to reconstruct Gd-enhanced MRA images of the carotid arteries with isotropic 1.25 mm resolution. It took approximately 30 seconds for a single R10000 processor (Silicon Graphics, Inc., Mountain View, Calif.) to perform this computation with a QR factorization algorithm. In many applications, this computation may have to be performed only once for a given patient; i.e. it need not be repeated on a slice-by-slice basis if the k-space sampling and prior knowledge are the same for all slices. However, the expense of this computation increases rapidly with the matrix dimension. Therefore, it could become a limiting factor if the prior knowledge is not strong enough to effectively limit the number of basis functions.

Detailed Description Text (68):

Notice that mrMRI utilizes prior knowledge of the approximate locations of but no assumptions are made about the configurations of those edges. Therefore, mrMRI is less model-dependent than methods which assume that the edge configurations of the unknown image are similar to those of prior images of the subject. For example, in one prior publication entitled "Reduced encoding Imaging by Generalized series Reconstruction" (RIGR), the \underline{image} is expressed in terms of a small number of basis functions that are products of slowly varying Fourier functions and a high resolution baseline <u>image</u> of the subject's anatomy. Therefore, all <u>edges</u> in a RIGR image must have the same configuration as the edges in the anatomical reference image, and problems can be expected if the unknown image contains new sharp edges. In "Feature-Recognizing MRI", a reduced basis set is identified as the principal components of "training" <u>images</u> of other subjects, who are thought to resemble the unknown subject. <u>Images</u> of the unknown subject are found by <u>computing</u> the basis function coefficients from a reduced set of k-space samples. Of course, these will only be accurate to the extent to which the unknown subject resembles the collection of training subjects. Furthermore, both "feature-recognizing" and RIGR images will suffer from noise amplification because the computation of basis function coefficients is usually not well-conditioned. In "Singular Value Decomposition MRI" (SVD MRI), a reduced basis set is derived from the singular value decomposition (SVD) of a single prior image of the subject. This is mathematically equivalent to applying the "feature-recognizing" procedure to the collection of columns in that \underline{image} . Other investigators have found that this method is model-dependent in the following sense: the SVD basis functions may not accurately represent new edges which are present in the image of interest but were not present in the prior image. Furthermore, SVD MRI also suffers from inherently low SNR. Zientara et al implemented SVD MRI by using direct RF excitation to encode signals with the profiles of the basis functions. In this way, the object's projection onto each basis function can be measured directly, and it is possible to avoid the ill-conditioned computation of the basis function coefficients from Fourier signals. Unfortunately, direct excitation requires the use of variable flip angles across the excitation profile, and this may produce 3-4 times less signal than that obtained with a uniform flip angle excitation followed by Fourier

Detailed Description Text (70):

In another illustrated embodiment, the method of reconstructing images is extended to time dependent signals. As used herein, a time dependent signal may be any information-containing signal transmitted in the radio frequency, microwave, infrared, or visible range.

<u>Detailed Description Text</u> (71):

The process of reconstructing time dependent signals is very similar to reconstruction of MR and other <u>images</u>. For example, MR <u>images</u> are reconstructed from samples of the <u>image's</u> Fourier representation at certain locations in the Fourier <u>space</u> (k-space). The frequency representation of a time dependent signal can be considered to be a one-dimensional <u>image</u>. The Fourier representation of that 1D <u>image</u> is the time dependent signal itself. Just as in MRI, such a 1D <u>image</u> can be reconstructed from samples of its Fourier representation at certain locations in the Fourier <u>space</u>; in other words, the signal's <u>frequency</u> representation can be reconstructed from samples of the time dependent signal at certain times. Then, the resulting frequency representation of the signal can be Fourier transformed to

14 of 20 10/27/2003 9:01 AM

reconstruct the time-dependent signal at any time.

Detailed Description Text (72):

The method of sampling and reconstructing time dependent signals may be used to transmit, receive, and reconstruct signals that have frequency components in multiple, possibly non-adjacent frequency bands. For example, it may be desirable to transmit a certain amount of information to a receiver over a certain period of time. However, there may not be an available band of frequency that is broad enough to permit the information to be transmitted in the desired time interval. If a sufficient number of narrow bands of frequency are available, the described invention makes it possible to use those multiple narrow frequency bands to transmit the information in the desired time interval. This process is described in the following example.

Detailed Description Text (76):

The receiving unit would use the known locations and breadths of the narrow frequency bands to determine the times at which the filtered signal should be sampled digitally. In general, the temporal sampling pattern would be comprised of a superposition of coarse sampling patterns. Each such coarse pattern would be suitable for Fourier transform reconstruction of any signal with frequency components in just one of the narrow bands. Also, each such coarse pattern would have a different temporal off -set, such off -set being chosen in order to make the eigenvalues of the reconstruction matrix comparable to one another.

Detailed Description Text (78):

The receiving unit would Fourier transform <u>subsets</u> of the stored sampled data and use the reconstruction matrix to linearly combine those Fourier transforms in order to reconstruct the signal's frequency components in each narrow frequency band.

Detailed Description Text (80):

A specific embodiment of a novel method and apparatus for reconstructing images according to the present invention has been described for the purpose of illustrating the manner in which the invention is made and used. It should be understood that the implementation of other variations and modifications of the invention and its various aspects will be apparent to one skilled in the art, and that the invention is not limited by the specific embodiments described. Therefore, it is contemplated to cover the present invention any and all modifications, variations, or equivalents that fall within the true spirit and scope of the basic underlying principles disclosed and claimed herein.

Other Reference Publication (1):

Beaty, M.G., et al., Derivative Sampling for Multiband Signals, Numer. Funct. Anal. and Optimiz., 20(9&10), 875-898 (1989).

Other Reference Publication (3):

Beatty, M.G., Multichannel sampling for multiband signals, 36 Signal Processing 133-138 (1994).

Other Reference Publication (13):

Walter, G.G., Recent Extension of the Sampling Theorem, Signal Processing, Part I: Signal Processing Theory (Auslander et al., eds.) 229-238 (Springer-Verlag, 1990).

CLAIMS:

1. A method of acquiring and reconstructing an <u>image</u>, such method comprising the <u>steps</u> of:

obtaining prior knowledge of the image, possibly by coarse sampling of the image; using the obtained prior knowledge of the image to identify relative locations of structures having relatively high contrast edges;

prescribing a <u>set of k-space</u> locations based upon the relative locations of the structures in order to achieve comparable eigenvalues of a reconstruction matrix;

sampling the k-space at the prescribed k-space locations to obtain k-space sample

15 of 20

data;

decomposing the k-space sample data into background data and edge data;

Fourier transforming the background data to reconstruct a background image
component;

Fourier transforming <u>subsets of the edge</u> data and using the reconstruction matrix to form a linear combination of these Fourier transformations in order to reconstruct an edge image component; and

combining the background $\underline{\text{image}}$ component and the $\underline{\text{edge image}}$ component to generate a final image.

- 2. The method of acquiring and reconstructing an <u>image</u> as in claim 1 further comprising selecting a grid-like pattern of cells which substantially segregates high contrast areas, having the high contrast edges, from other areas.
- 3. The method of acquiring and reconstructing an \underline{image} as in claim 2 further comprising prescribing a $\underline{plurality}$ of \underline{k} -space $\underline{sampling}$ patterns for the high contrast areas and for the other areas, one of such \underline{k} -space $\underline{sampling}$ patterns comprising a dense collection of \underline{k} -space locations near the center of \underline{k} -space, and \underline{each} of the other such \underline{k} -space $\underline{sampling}$ patterns comprising a coarse grid of \underline{k} -space locations covering a relatively large region of \underline{k} -space, each such coarse grid being suitable for Fourier transform reconstruction of any \underline{image} having features in just one cell and each such coarse grid having a pre-determined off $\underline{-set}$ in \underline{k} -space.
- 4. The method of acquiring and reconstructing an <u>image</u> as in claim 3 further comprising determining the reconstruction matrix based upon the locations of the segregated high contrast areas and the off <u>-sets</u> of the prescribed coarse <u>k-space</u> sampling patterns.
- 5. The method of acquiring and reconstructing an image as in claim 4 further comprising computing the eigenvalues of the determined reconstruction matrix.
- 6. The method of acquiring and reconstructing an <u>image</u> as in claim 5 further comprising adjusting the off <u>-sets</u> of the prescribed coarse <u>k-space</u> sampling patterns so that the <u>computed</u> eigenvalues of the determined reconstruction matrix are approximately equal.
- 7. The method of acquiring and reconstructing an image as in claim 6 further comprising sampling the data at all of the locations in all of the prescribed dense and coarse k-space sampling patterns.
- 8. The method of acquiring and reconstructing an <u>image</u> as in claim 7 further comprising multiplying data at the locations of the dense <u>k-space</u> pattern by values corresponding to a low-pass filter to provide low-pass filtered data.
- 9. The method of acquiring and reconstructing an <u>image</u> as in claim 7 further comprising multiplying data at the locations of the coarse <u>k-space</u> sampling patterns by values corresponding to a complementary high-pass filter to provide high-pass filtered data.
- 10. The method of acquiring and reconstructing an \underline{image} as in claim 8 further comprising Fourier transforming the low-pass filtered data to reconstruct the background \underline{image} component.
- 11. The method of acquiring and reconstructing an <u>image</u> as in claim 9 further comprising Fourier transforming the high-pass filtered data of each coarse <u>k-space</u> sampling pattern and using the reconstruction matrix to linearly combine the Fourier transforms to reconstruct the edge component of the <u>image</u>.
- 12. The method of acquiring and reconstructing an <u>image</u> as in claim 11 further comprising adding the background <u>image</u> component to the <u>edge image</u> component to reconstruct the <u>image</u>.

16 of 20 10/27/2003 9:01 AM

13. A method of digitizing and reconstructing a time-dependent signal, such method comprising the $\underline{\text{steps}}$ of:

obtaining prior knowledge of frequencies at which the signal has Fourier components which exceed a threshold, possibly by filtering the signal to remove or reduce all other undesired frequency components;

using the obtained prior knowledge to prescribe a set of times in order to achieve comparable eigenvalues of a reconstruction matrix;

sampling the signal at the prescribed times in order to obtain data;

Fourier transforming <u>subsets</u> of the sampled data and using the reconstruction matrix to form a linear combination of these Fourier transformations in order to reconstruct the signal's Fourier components in each frequency band; and

inverse Fourier transforming the reconstructed Fourier components in each frequency band in order to reconstruct the time-dependent signal having frequencies in each frequency band.

- 15. The method of digitizing and reconstructing a time-dependent signal as in claim 14 further comprising prescribing a <u>plurality</u> of temporal sampling patterns for the spectral bands having frequency activity, each such temporal pattern consisting of a coarse pattern of times which pattern is suitable for Fourier transform reconstruction of the frequency components of any signal having just one frequency band and which pattern has a predetermined off -set in time.
- 16. The method of digitizing and reconstructing a time-dependent signal as in claim 15 further comprising determining the reconstruction matrix depending on the frequency locations of the segregated spectral bands and the time off -sets of the prescribed coarse temporal sampling patterns.
- 17. The method of digitizing and reconstructing a time-dependent signal as in claim 16 further comprising computing the eigenvalues of the determined reconstruction matrix.
- 18. The method of digitizing and reconstructing a time-dependent signal as in claim 17 further comprising adjusting the prescribed time off <u>sets</u> so that the <u>computed</u> eigenvalues of the determined reconstruction matrix are approximately equal.
- 22. Apparatus for acquiring and reconstructing an image, such apparatus comprising:

means for obtaining prior knowledge of the <u>image</u>, possibly by coarse sampling of the <u>image</u>; using the obtained prior knowledge of the <u>image</u> to identify relative locations of structures having relatively high contrast edges;

means for prescribing a $\underline{\text{set of }k\text{-space}}$ locations based upon the relative locations of the structures in order to achieve comparable eigenvalues of a reconstruction matrix;

means for sampling the \underline{k} -space at the prescribed \underline{k} -space locations to obtain \underline{k} -space sample data;

means for decomposing the k-space sample data into background data and edge data;

means for Fourier transforming the background data to reconstruct a background image component;

means for Fourier transforming <u>subsets of the edge</u> data and using the reconstruction matrix to form a linear combination of these Fourier transformations in order to reconstruct an edge image component; and

means for combining the background \underline{image} component and the \underline{edge} \underline{image} component to generate a final \underline{image} .

- 23. The <u>apparatus</u> for acquiring and reconstructing an <u>image</u> as in claim 22 further comprising means for selecting a grid-like pattern of cells which substantially segregates high contrast areas, having the high contrast edges, from other areas.
- 24. The <u>apparatus</u> for acquiring and reconstructing an <u>image</u> as in claim 23 further comprising means for prescribing a <u>plurality of k-space</u> sampling patterns for the high contrast areas and for the other areas, one of such <u>k-space</u> sampling patterns comprising a dense collection of <u>k-space</u> locations near the center of <u>k-space</u>, and <u>each of the other such k-space</u> sampling patterns comprising a coarse grid of <u>k-space</u> locations covering a relatively large region of <u>k-space</u>, each such coarse grid being suitable for Fourier transform reconstruction of any <u>image</u> having features in just one cell and each such coarse grid having a pre-determined off <u>-set in k-space</u>.
- 25. The <u>apparatus</u> for acquiring and reconstructing an <u>image</u> as in claim 24 further comprising means for determining the reconstruction matrix based upon the locations of the segregated high contrast areas and the off -sets of the prescribed coarse k-space sampling patterns.
- 26. The <u>apparatus</u> for acquiring and reconstructing an <u>image</u> as in claim 25 further comprising means for <u>computing</u> the eigenvalues of the determined reconstruction matrix.
- 27. The apparatus for acquiring and reconstructing an \underline{image} as in claim 26 further comprising means for adjusting the off $\underline{-sets}$ of the prescribed coarse $\underline{k-space}$ sampling patterns so that the $\underline{computed}$ eigenvalues of the determined reconstruction matrix are approximately equal.
- 28. The <u>apparatus</u> for acquiring and reconstructing an \underline{image} as in claim 27 further comprising means for sampling the data at all of the locations in all of the prescribed dense and coarse k-space sampling patterns.
- 29. The <u>apparatus</u> for acquiring and reconstructing an <u>image</u> as in claim 28 further comprising means for multiplying data at the locations of the dense <u>k-space</u> pattern by values corresponding to a low-pass filter to provide low-pass filtered data.
- 30. The <u>apparatus</u> for acquiring and reconstructing an <u>image</u> as in claim 29 further comprising means for multiplying data at the locations of the coarse <u>k-space</u> sampling patterns by values corresponding to a complementary high-pass filter to provide high-pass filtered data.
- 31. The apparatus for acquiring and reconstructing an \underline{image} as in claim 29 further comprising means for Fourier transforming the low-pass filtered data to reconstruct the background \underline{image} component.
- 32. The apparatus for acquiring and reconstructing an \underline{image} as in claim 30 further comprising means for Fourier transforming the high-pass filtered data of each coarse \underline{k} -space sampling pattern and using the reconstruction matrix to linearly combine the Fourier transforms to reconstruct the \underline{edge} component of the \underline{image} .
- 33. The <u>apparatus</u> for acquiring and reconstructing an <u>image</u> as in claim 32 further comprising means for adding the background <u>image</u> component to the <u>edge image</u> component to reconstruct the image.
- 34. Apparatus for digitizing and reconstructing a time-dependent signal, such apparatus comprising:

means for obtaining prior knowledge of the frequencies at which the signal has significantly large Fourier components, possibly by filtering the signal to remove or reduce all other frequency components;

means for using the obtained prior knowledge to prescribe a set of times in order to achieve comparable eigenvalues of a reconstruction matrix;

means for sampling the signal at the prescribed times in order to obtain data;

means for Fourier transforming <u>subsets</u> of the sampled data and using the reconstruction matrix to form a <u>linear</u> combination of these Fourier transformations in order to reconstruct the signal's Fourier components in each frequency band; and

means for inverse Fourier transforming the reconstructed Fourier components in each frequency band in order to reconstruct the time-dependent signals with frequencies in each frequency band.

- 35. The <u>apparatus</u> for digitizing and reconstructing a time-dependent signal as in claim 34 further comprising means for selecting a spectral pattern which substantially segregates spectral bands having frequency activity above a predetermined threshold, from other areas.
- 36. The <u>apparatus</u> for digitizing and reconstructing a time-dependent signal as in claim 35 further comprising means for prescribing a <u>plurality</u> of temporal sampling patterns for the spectral bands having frequency activity, each such temporal pattern consisting of a coarse pattern of times which pattern is suitable for Fourier transform reconstruction of the frequency components of any signal having just one frequency band and which pattern has a predetermined off -set in time.
- 37. The <u>apparatus</u> for digitizing and reconstructing a time-dependent signal as in claim 36 further comprising means for determining the reconstruction matrix depending on the frequency locations of the segregated spectral bands and the time off<u>-sets</u> of the prescribed coarse temporal sampling patterns.
- 38. The <u>apparatus</u> for digitizing and reconstructing a time-dependent signal as in claim 37 further comprising means for <u>computing</u> the eigenvalues of the determined reconstruction matrix.
- 39. The <u>apparatus</u> for digitizing and reconstructing a time-dependent signal as in claim 38 further comprising means for adjusting the prescribed time off <u>sets</u> so that the <u>computed</u> eigenvalues of the determined reconstruction matrix are approximately equal.
- 40. The <u>apparatus</u> for digitizing and reconstructing a time-dependent signal as in claim 39 further comprising means for using an analogue or digital filter to suppress signals with frequency components outside the segregated spectral bands and for sampling the filtered signal at all locations in all of prescribed coarse temporal sampling patterns and for storing the sampled data.
- 41. The <u>apparatus</u> for digitizing and reconstructing a time-dependent signal as in claim 40 further comprising means for Fourier transforming the sampled data in each coarse temporal sampling pattern and using the reconstruction matrix to linearly combine the Fourier transforms to reconstruct the frequency components in each frequency band.
- 42. The <u>apparatus</u> for digitizing and reconstructing a time-dependent signal as in claim 41 further comprising means for inverse Fourier transforming the reconstructed frequency components in each frequency band in order to reconstruct the time-dependent signals having frequencies in each frequency band.
- 43. Apparatus for digitizing and reconstructing a time-dependent signal, such apparatus comprising:
- a <u>scanning</u> receiver which obtains prior knowledge of the frequencies at which the signal has significantly large Fourier components, possibly by filtering the signal to remove or reduce all other frequency components;
- a matrix <u>processor</u> which uses the obtained prior knowledge to prescribe a <u>set</u> of times in order to achieve comparable eigenvalues of a reconstruction matrix;
- an analogue or digital filtering <u>processor</u> which suppresses signals with frequency components outside the spectral bands of interest;

- a sampling <u>processor</u> which samples the filtered signal at the prescribed times in order to obtain data and which stores the sampled data;
- a Fourier <u>processor</u> which Fourier transforms <u>subsets</u> of the sampled data and uses the reconstruction matrix to form a linear combination of these Fourier transformations in order to reconstruct the signal's Fourier components in each frequency band; and

an inverse Fourier <u>processor</u> which inverse Fourier transforms the reconstructed Fourier components in each frequency band in order to reconstruct the time-dependent signals in each frequency band.

- 44. The $\underline{apparatus}$ for digitizing and reconstructing a time-dependent signal as in claim 43 further comprising a wide-band receiver.
- 45. The <u>apparatus</u> for digitizing and reconstructing a time-dependent signal as in claim 44 further comprising an analog or digital filter which suppresses radio frequency energy outside desired spectral ranges.
- 46. The <u>apparatus</u> for digitizing and reconstructing a time-dependent signal as in claim 45 further comprising a sampling $\underline{\text{device}}$ which samples the filtered signal at the prescribed times, and stores the resulting data.
- 47. The <u>apparatus</u> for digitizing and reconstructing a time-dependent signal as in claim 46 further comprising a reconstruction <u>processor</u> which reconstructs the time-dependent signal, which has frequency components in each frequency band, from the sampled data.

Generate Collection

Print

L19: Entry 80 of 84

File: USPT

Jul 27, 1999

DOCUMENT-IDENTIFIER: US 5928148 A

TITLE: Method for performing magnetic resonance angiography over a large field of view using table stepping

Abstract Text (1):

MRA data is acquired from a large region of interest by translating the patient to successive stations at which successive portions of the MRA data set are acquired. Patient movement is chosen to track a bolus of contrast agent as it passes through the region of interest to achieve maximum image contrast. In one embodiment a stationary local coil is supported adjacent the patient to acquire the MRA data and in another embodiment a multi-segment local coil moves with the patient and its segments are sequentially switched into operation.

Parent Case Text (2):

This application is based on provisional application Ser. No. 60/048,286, filed on Jun. 2, 1997 and entitled "METHOD FOR PERFORMING MAGNETIC RESONANCE ANGIOGRAPHY OVER A LARGE FIELD OF VIEW USING TABLE STEPPING".

Brief <u>Summary Text</u> (3):

Diagnostic studies of the human vasculature have many medical applications. X-ray imaging methods such as digital subtraction angiography ("DSA") have found wide use in the visualization of the cardiovascular system, including the heart and associated blood vessels. One of the advantages of these x-ray techniques is that image data can be acquired at a high rate (i.e. high temporal resolution) so that a sequence of images may be acquired during injection of the contrast agent. Such "dynamic studies" enable one to select the image in which the bolus of contrast agent is flowing through the vasculature of interest. Images showing the circulation of blood in the arteries and veins of the kidneys, the neck and head, the extremities and other organs have immense diagnostic utility. Unfortunately, however, these x-ray methods subject the patient to potentially harmful ionizing radiation and often require the use of an invasive catheter to inject a contrast agent into the vasculature to be <u>imaged</u>. There is also the issue of increased nephro-toxicity and allergic reactions to iodinated contrast agents used in conventional x-ray angiography.

Brief Summary Text (4):

Magnetic resonance angiography (MRA) uses the nuclear magnetic resonance (NMR) phenomenon to produce images of the human vasculature. When a substance such as human tissue is subjected to a uniform magnetic field (polarizing field B.sub.0), the individual magnetic moments of the spins in the tissue attempt to align with this polarizing field, but precess about it in random order at their characteristic Larmor frequency. If the substance, or tissue, is subjected to a magnetic field (excitation field B.sub.1) which is in the x-y plane and which is near the Larmor frequency, the net aligned moment, M.sub.z, may be rotated, or "tipped", into the x-y plane to produce a net transverse magnetic moment M.sub.t. A signal is emitted by the excited spins, and after the excitation signal B.sub.1 is terminated, this signal may be received and processed to form an image.

Brief Summary Text (5):

When utilizing these signals to produce <u>images</u>, magnetic field <u>gradients</u> (G.sub.x G.sub.y and G.sub.z) are employed. Typically, the region to be <u>imaged is scanned</u> by a sequence of measurement cycles in which these <u>gradients</u> vary according to the

particular localization method being used. The resulting $\underline{\text{set}}$ of received NMR signals are digitized and $\underline{\text{processed}}$ to reconstruct the $\underline{\text{image}}$ using one of many well known reconstruction techniques.

Brief Summary Text (6):

MR angiography (MRA) has been an active area of research. Two basic techniques have been proposed and evaluated. The first class, time-of-flight (TOF) techniques, consists of methods which use the motion of the blood relative to the surrounding tissue. The most common approach is to exploit the differences in magnetization saturation that exist between flowing blood and stationary tissue. Flowing blood, which is moving through the excited section, is continually refreshed by spins experiencing fewer excitation pulses and is, therefore, less saturated. The result is the desired <u>image</u> contrast between the high-signal moving blood and the low-signal stationary tissues.

Brief Summary Text (7):

MRA methods have also been developed that encode motion into the phase of the acquired signal as disclosed in U.S. Pat. No. Re. 32,701. These form the second class of MRA techniques and are known as phase contrast (PC) methods. Currently, most PC MRA techniques acquire two images, with each images having a different sensitivity to the same velocity component. Angiographic images are then obtained by forming either the phase difference or complex difference between the pair of velocity-encoded images.

Brief Summary Text (8):

To enhance the diagnostic capability of MRA a contrast agent such as gadolinium can be injected into the patient prior to the MRA scan. Excellent diagnostic images may be acquired using contrast-enhanced MRA if the data acquisition is properly timed with the bolus passage.

Brief Summary Text (9):

The non-invasiveness of MRA makes it a valuable screening tool for cardiovascular diseases. Screening typically requires imaging vessels in a large volume. This is particularly true for diseases in the runoff vessels of the lower extremity. The field of view (FOV) in MR imaging is limited by the volume of the B.sub.0 field homogeneity and the receiver coil size (typically, the FOV<48 cm on current commercial MR scanners). The anatomic region of interest in the lower extremity, for example, is about 100 cm and this requires several FOVs, or stations, for a complete study. This requires that the patient be repositioned inside the bore of the magnet, the patient be relandmarked, scout images be acquired and a preparation scan be performed for each FOV. All of these additional steps take time and, therefore, are expensive. When contrast enhanced MRA is performed, the repositioning also necessitates additional contrast injections.

Brief Summary Text (11):

The present invention is a method for acquiring NMR data from a large region of interest by acquiring NMR data from a series of smaller fields of view which collectively span the large region of interest. The patient is automatically translated, or stepped, to a new position within the bore of the magnet by moving the patient table between the acquisition of each field of view. Scan parameters remain constant throughout the procedure and the separate reconstructed images are registered and combined to provide a single image of the large region of interest.

Brief Summary Text (12):

Another aspect of the present invention is to acquire the entire region of interest with one injection of contrast agent. The acquisition of each field of view is timed to correspond with the peak image contrast produced by the bolus of contrast agent. The order in which the separate fields of view are acquired and the speed of the patient translation between fields of view are selected to track the peak intraarterial contrast as the bolus transits through the region of interest.

Brief Summary Text (13):

Yet another aspect of the present invention is the use of local coils to improve the signal-to-noise ratio of the acquired MRA image. In one embodiment an array of local coils are positioned adjacent the patient and span the large region of interest.

This local coil array moves with the patient as the table is translated from one station to the next, and successive segments of the array are connected to the receiver as they move into the $\underline{imaging}$ field of view. In a second embodiment a stationary local coil is supported adjacent the patient in the $\underline{imaging}$ field of view. The patient is translated through the $\underline{imaging}$ field of view and the stationary reception field of the local coil.

Brief Summary Text (14):

A general object of the invention is to efficiently acquire MRA data from a large region of interest. A single scan is performed in which MRA data is acquired from successive parts of the large region of interest. This is accomplished by translating the patient between acquisitions and concatenating the acquired data to form a single image of the entire region of interest.

Brief Summary Text (15):

Another object of the invention is to provide optimal contrast by timing the acquisition of MRA data with the arrival of contrast agent at each successive FOV in the region of interest. This is accomplished by acquiring data from which the velocity of the contrast agent bolus as it transits the region of interest is estimated. This velocity estimate is used to control the rate at which the patient is translated to successive FOVs during the scan and to track the peak in the contrast produced by the bolus.

Brief Summary Text (16):

Yet another object of the invention is to improve the SNR of the acquired <u>image</u>. This is accomplished by using a local coil which is positioned adjacent the patient. In one embodiment the local coil remains stationary as the patient is translated by it during the <u>scan</u>. In another embodiment a multi-segment local coil is carried by the patient. The local coil segments are successively switched into operation as the patient translates through the bore during the scan.

Drawing Description Text (7):

FIG. 6 is a flow chart of the sequence of steps performed by the MRI system of FIG. 1 to practice the preferred embodiment of the invention;

Detailed Description Text (2):

Referring first to FIG. 1, there is shown the major components of a preferred MRI system which incorporates the present invention. The operation of the system is controlled from an operator console 100 which includes a keyboard and control panel 102 and a display 104. The console 100 communicates through a link 116 with a separate computer system 107 that enables an operator to control the production and display of images on the screen 104. The computer system 107 includes a number of modules which communicate with each other through a backplane. These include an image processor module 106, a CPU module 108 and a memory module 113, known in the art as a frame buffer for storing image data arrays. The computer system 107 is linked to a disk storage 111 and a tape drive 112 for storage of image data and programs, and it communicates with a separate system control 122 through a high speed serial link 115.

Detailed Description Text (3):

The system control 122 includes a set of modules connected together by a backplane. These include a CPU module 119 and a pulse generator module 121 which connects to the operator console 100 through a serial link 125. It is through this link 125 that the system control 122 receives commands from the operator which indicate the scan sequence that is to be performed. The pulse generator module 121 operates the system components to carry out the desired scan sequence. It produces data which indicates the timing, strength and shape of the RF pulses which are to be produced, and the timing of and length of the data acquisition window. The pulse generator module 121 connects to a set of gradient amplifiers 127, to indicate the timing and shape of the gradient pulses to be produced during the scan. The pulse generator module 121 also receives patient data from a physiological acquisition controller 129 that receives signals from a number of different sensors connected to the patient, such as ECG signals from electrodes or respiratory signals from a bellows. And finally, the pulse generator module 121 connects to a scan room interface circuit 133 which receives signals from various sensors associated with the condition of the patient

and the magnet system. It is also through the \underline{scan} room interface circuit 133 that a patient positioning system 134 receives commands from the pulse generator module 121 to move the patient to the sequence of desired positions to perform the \underline{scan} in accordance with the present invention. The operator can thus control the operation of the patient positioning system 134 through the keyboard and control panel 102.

Detailed Description Text (4):

The <u>gradient</u> waveforms produced by the pulse generator module 121 are applied to a <u>gradient</u> amplifier system 127 comprised of G.sub.x, G.sub.y and G.sub.z amplifiers. Each <u>gradient</u> amplifier excites a corresponding <u>gradient</u> coil in an assembly generally designated 139 to produce the magnetic field <u>gradients</u> used for position <u>encoding</u> acquired signals. The <u>gradient</u> coil assembly 139 forms part of a magnet assembly 141 which includes a polarizing magnet 140 and a <u>whole-body RF coil 152.</u> A transceiver module 150 in the system control 122 produces pulses which are amplified by an RF amplifier 151 and coupled to the RF coil 152 by a transmit/receive switch 154. The resulting signals radiated by the excited nuclei in the patient may be sensed by the same RF coil 152 and coupled through the transmit/receive switch 154 to a preamplifier 153. The amplified NMR signals are demodulated, filtered, and digitized in the receiver section of the transceiver 150.

Detailed Description Text (5):

The transmit/receive switch 154 is controlled by a signal from the pulse generator module 121 to electrically connect the RF amplifier 151 to the coil 152 during the transmit mode and to connect the preamplifier 153 during the receive mode. The transmit/receive switch 154 also enables a separate RF local coil to be used during the receive mode. In the preferred embodiment of the invention a single, stationary local coil described below and shown in FIG. 7 is switched into operation. In the alternative, a multi-segment local coil described below and shown in FIG. 8 may also be used. In this case, the separate segments of the local coil are switched into operation by the transmit/receive switch 154 as the patient is translated to successive stations during the scan.

Detailed Description Text (6):

The NMR signals picked up by the RF local coil are digitized by the transceiver module 150 and transferred to a memory module 160 in the system control 122. When the scan is completed and an entire array of data has been acquired in the memory module 160, an array processor 161 operates to Fourier transform the data into an array of image data. This image data is conveyed through the serial link 115 to the computer system 107 where it is stored in the disk memory 111. In response to commands received from the operator console 100, this image data may be archived on the tape drive 112, or it may be further processed by the image processor 106 and conveyed to the operator console 100 and presented on the display 104.

Detailed Description Text (8):

While many pulse sequences may be used to practice the present invention, in the preferred embodiment a 2D gradient -recalled echo pulse sequence is used to acquire the NMR data. Referring particularly to FIG. 2, an RF excitation pulse 220 having a flip angle of 50.degree. is produced in the presence of a slab select gradient pulse 222 to produce transverse magnetization in the 2D slab of interest (typically 100 to 150 mm thick). This is followed by a phase encoding gradient pulse 226 directed along the y axis. A readout gradient pulse 228 directed along the x axis follows and a partial echo (60%) NMR signal 230 is acquired and digitized as described above. After the acquisition, a spoiler gradient pulse 232 is applied along the z axis and a rewinder gradient pulse 234 is applied to rephase the magnetization before the pulse sequence is repeated as taught in U.S. Pat. No. 4,665,365.

Detailed Description Text (9):

As is well known in the art, the pulse sequence is repeated and the phase encoding
pulse 226 is stepped through a series of values to sample the 2D k-space in the field of view. In the preferred embodiment 256 phase encodings are employed along the y axis. Sampling along the k.sub.x axis is performed by sampling the echo signal 230 in the presence of the readout gradient pulse 228 during each pulse sequence. It will be understood by those skilled in the art that only a partial sampling along the k.sub.x axis is performed and the missing data is computed using a homodyne reconstruction or by zero filling. This enables the echo time (TE) of the pulse

sequence to be shortened to less than 1.8 to 2.0 ms and the pulse repetition rate (TR) to be shortened to less than 10.0 msecs.

Detailed Description Text (10):

Referring to FIG. 3, an examination of the vasculature of a patient's legs can be performed by dividing up the region of interest into three overlapping fields of view indicated at 250, 252 and 254. As shown in FIG. 4, this is accomplished by moving a patient table 256 to three successive locations, or stations, within the bore of the magnet to align the respective centers of the field of view with the isocenter 258 of the MRI system. A local RF coil 262 such as a 4-coil array consisting of anterior and posterior subunits is positioned at the system isocenter and it remains stationary as the patient is translated by the table 256 to three different stations. At each station of the table 256 the pulse sequence of FIG. 2 is employed to acquire NMR data from which an image of the field of view may be reconstructed.

Detailed Description Text (11):

As shown in FIG. 7, a coil holder 200 has a closed end 202 which is attached to the carriage cover of the MRI system and supports an upper plate 204 and lower plate 206 which extend into the bore of the magnet, The end of the upper plate 204 supports the upper RF coil unit 262A which rests on the patient and slides smoothly over the patient during table translation. A rectangular opening 207 in the upper plate 204 provides space for the patient's feet. The lower plate 206 supports the lower RF coil unit 262B on its outer end which is positioned beneath the patient. The patient lies on an elevated table 208 and the lower plate 206 extends beneath the elevated table 208. The elevated table 208 rests on the sliding table 210 in the MRI system and is spaced therefrom by legs 212 to provide space for the lower plate 206. The patient may thus be translated between the RF coil units 262A and B which remain stationary at the system isocenter and in close proximity for optimal signal reception at all table stations.

Referring to FIGS. 9A and 9B, this alternative local coil is a coil array comprised of five coil segments 214-218, each comprised of four coil elements. The coil segments 214-218 are positioned on the patient and distributed along the entire region of interest to be imaged -- in this case, the legs and feet. The coil elements are supported by fabric (not shown) which is sewn into a pant-like garment that clothes the patient's legs.

Detailed Description Text (13):

Each coil segment 214-218 has four coil elements that acquire NMR data from the Two of the coil elements are positioned on top, or anterior, of the lower extremity as seen in FIG. 9B, and the other two elements are positioned below, or posterior, of the lower extremity. The coil elements connect together to form one of the coil segments 214-218, and each is separately connected through terminals 219 to the above-described transmit/receive switch 154. Coupling between coil segments 214-218 is of little concern, because only one segment is operative at any moment during the scan. As the patient is translated to bring the successive coil segments 214-218 into the FOV of the MRI system, the aligned coil segment is connected to the system transceiver module 150. MRA data is acquired using that coil segment and the patient is then translated to the next station and the next coil segment is enabled.

Detailed Description Text (14):

The multi-element coil segments may be constructed using a number of well-known methods. Coupling between the separate coil elements is minimized to increase the SNR of the data acquired using the coil segment. Such decoupling is achieved using the methods taught in U.S. Pat. No. 4,825,162 issued to Roemer, et al., and entitled "Nuclear Magnetic Resonance (NMR) Imaging With Multiple Surface Coils" or U.S. Pat. No. 4,721,913 issued to Hyde, et al. and entitled "NMR Local Coil Network".

Detailed Description Text (15):

As shown in FIG. 6, the scan is performed under the direction of a stored program which directs the pulse generator module 121 to carry out a sequence of indicated by process block 370, the pulse control module 121 sends command signals

to the patient positioning system 134 which moves the table to align the first $\frac{FOV}{A}$ at the system isocenter 258. A loop is then entered in which NMR data is acquired for a $\frac{complete image}{A}$. More specifically, the pulse control module 121 directs the MRI system to perform the pulse sequence of FIG. 2 to acquire one view of NMR data as indicated at $\frac{process}{A}$ block 372. Phase $\frac{encodings}{A}$ are stepped as described above and additional views are acquired until all of $\frac{k-space}{A}$ has been sampled and the acquisition is $\frac{encodings}{A}$.

Detailed Description Text (16):

At the completion of the first image acquisition the pulse control module 121 commands the patient positioning system 134 to move the table 256 to the next station to align the next field of view at the system isocenter 258 as indicated at process block 376. In the preferred embodiment this distance is 25 cm. Another image is then acquired at 372 and 374. This sequence of acquiring an image and moving the patient table 256 continues until the last field of view in the scan has been acquired as determined at decision block 378. Both the FOV sizes and the separation between the anterior and posterior coils may vary from FOV to FOV for optimal image resolution and signal-to-noise ratio.

Detailed Description Text (17):

The acquired field of view <u>images</u> are registered with each other and combined to form a single <u>image</u> of the much larger region of interest. The patient is immobilized to the table 256 with straps (not shown) to minimize misregistration between the field of view <u>images</u>. In addition, a marker made of a contrast agent solution which produces a high level signal can be placed along side the patient and used to align each field of view <u>image</u> such that they are in registration with each other and form a single, contiguous <u>image</u> of the entire region of interest.

Detailed Description Text (18):

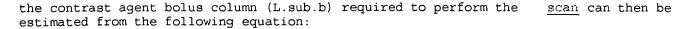
In the preferred method the acquisition of each FOV is timed to occur when maximum image contrast is produced by a contrast agent administered intravenously to the patient. A test bolus (eg. 5 ml of gadolinium) is administered intravenously to measure the bolus timing curve at a predetermined region of interest, typically the second FOV. As shown in FIG. 5, for example, the curve 274 peaks in the first FOV 250 at approximately 23 seconds after the contrast agent is administered, the curve 275 peaks in the second FOV 252 at approximately 29 seconds after the contrast agent is administered and the curve 276 peaks in the third FOV 254 at approximately 35 seconds after contrast administration. This establishes when the data should be acquired for best image contrast.

Detailed Description Text (19):

If the three FOVs 250, 252, 254 are acquired in order, the intraarterial column of contrast agent is imaged as it transits through the patient's legs. To maximize image contrast, the velocity of the bolus movement is estimated and the table translation is timed to acquire each FOV at peak contrast. One way to estimate the bolus velocity is to measure the arterial velocity (averaged over the cardiac cycle) by acquiring a phase contrast image through the artery of interest in the center of the region of interest as described in U.S. Pat. No. Re 32,701. Blood flow velocity can be determined from this image and an estimate made of the bolus velocity. Another way to estimate the bolus velocity is to perform a timing scan in which the bolus advancement through the $\begin{subarray}{c} FOV \end{subarray}$ is monitored using a high temporal frame rate. This second method provides a rapid estimation of bolus velocity that is accurate enough to use with the present invention. From this velocity estimate and the peak contrast timing for the central FOV 252, the timing for the acquisition of the 250 and 254 can be calculated. These timings will determine the rate of table translation between FOV acquisitions.

Detailed Description Text (20):

The timing for table translation is estimated from three parameters: the estimate of bolus velocity; the duration of data acquisition at each FOV; and the time for moving the patient from one FOV to the next. Optimal results are achieved in the preferred embodiment if the leading edge of the bolus contrast agent has flowed into the next FOV for about 5 sec (T.sub.12). The time for each additional FOV (T.sub.s) is the time for table translation from one FOV to the next (3 seconds or less if performed manually), and the imaging duration (about 5-7 sec). The total length of



Detailed <u>Description Text</u> (21):

Here N.sub.s is the number of FOVs to be imaged, and V.sub.b is the estimated bolus velocity. L.sub.s is the table translation distance between stations, which is slightly smaller than FOV to provide overlapping acquisitions between adjacent stations. A constant bolus velocity is used in the above equation. This concept can also be extended straight forwardly to the case of varying bolus velocity using integration. The imaging duration at each station is kept at several seconds to account for velocity variation as the contrast column travels to the more peripheral FOVs. Accordingly, the contrast duration is T.sub.b =L.sub.b /V.sub.b and the injection duration is less than this by the cardiac dispersion effects (.tau..sub.c .about.5 seconds). For a given injection rate, (R.sub.i) the required contrast dose is as follows:

Detailed Description Text (22):

An example of using this timing and contrast dose information is illustrated in FIG. 8. In this example, the length of each <u>imaging</u> region is 25 cm and indicated by shaded region 290, and it is translated to the second, third and fourth <u>FOVs</u> at 30, 40 and 50 seconds respectively. The contrast agent bolus 292 transits the region at a speed of 3 cm/sec and <u>imaging</u> of the first <u>FOV</u> continues until the leading <u>edge</u> of the contrast agent bolus 292 is 5 seconds into the second <u>FOV</u>. The time at each additional <u>FOV</u> is 10 seconds, 7 seconds for acquiring <u>image</u> data and 3 seconds for moving the next <u>FOV</u> into the imaging region 290. The <u>total</u> length of the contrast agent bolus is 55 cm, which corresponds to a bolus duration of 18.3 seconds. A bolus injection duration of 15 seconds is used, and at an injection rate of 1 cc/sec., the total dose is 15 cc (using 3.3 sec .tau..sub.c).

Detailed Description Text (23):

As is well known in the art, "mask" <u>images</u> may also be acquired before contrast agent is administered. In the preferred embodiment, the mask <u>images</u> are acquired before bolus injection at each of the stations. The above described contrast enhanced acquisition is then performed and a complex subtraction of corresponding voxels in the mask <u>image</u> from the reconstructed <u>image</u> is performed to further enhance image quality.

Detailed Description Text (24):

The preferred method for practicing the invention includes conducting a "scout scan" to confirm that the vasculature of interest is within the FCV of at least one of the stations. This is followed by a "timing scan" in which information is acquired regarding the arrival and velocity of the contrast agent bolus, and by a "mask scan" in which the mask image data is acquired. And finally, the "bolus tracking MRA scan" is conducted as described above and shown in FIG. 6. The following is an exemplary procedure for carrying out these steps in a four station scan of a patient's legs.

<u>Detailed Description Text</u> (25): Scout Scan

Detailed Description Text (26):

A multiple location, sagittal acquisition using a 2D fast gradient echo sequence $(\underline{FOV}=40 \text{ cm}, \ TE/TR=2/9, \ receiver \ bandwidth=16 \ kHz, 256.times.256, 1/2 FOV, total acquisition time .about.15 sec) is performed at the first station. The patient is translated to the second station and the same <math>\underline{scan}$ is repeated immediately without any prescan. This $\underline{process}$ repeats until all stations are \underline{imaged} . For a 4-station scout \underline{scan} , the total $\underline{imaging}$ time is about 70 sec (allowing 10 seconds for each table motion).

<u>Detailed Description Text</u> (27): <u>Timing Scan</u>

Detailed Description Text (28):

A thick coronal <u>slab</u> timing acquisition is typically performed at the second station using a gadolinium contrast agent test dose (3-5 mL, at 1 mL/sec injection rate) and a 2D fast <u>gradient</u> echo sequence (FOV=32-40 cm, 130-170 mm thick, TE/TR=2/9,

receiver bandwidth=16 kHz, 256.times.160-192, 40-60 $\underline{\text{image}}$ frames, $\underline{\text{total}}$ acquisition time .about.60-90 sec to ensure the capture of the contrast peak). From this timing acquisition, the arrival time of the contrast agent in the $\underline{\text{FOV}}$ is measured, and the bolus velocity is estimated based on the time required for the bolus to transit the FOV.

Detailed Description Text (29):

Mask Scan

Detailed Description Text (30):

Similar to the timing \underline{scan} , a thick coronal \underline{slab} containing all arteries of interest is acquired using a fast $\underline{2D}$ $\underline{gradient}$ echo sequence ($\underline{FOV}=32$ cm, 130-170 mm thick, TE/TR=2/9, receiver bandwidth= $\underline{16}$ kHz, 256.times.160-192, 40-60 \underline{image} frames, total acquisition time .about.60-90 sec. In contrast to the timing \underline{scan} , the table is translated to each station at times determined by the timing \underline{scan} and mask data is acquired at each \underline{FOV} .

<u>Detailed Description Text</u> (31):

Bolus Tracking MRA Scan

Detailed Description Text (32):

The contrast agent is administered and a <u>scan</u> is conducted using the same prescription as the mask <u>scan</u>. As with the mask <u>scan</u>, the data acquisition is begun at the time, and the table is translated at the times determined by the timing scan.

Detailed Description Text (34):

Next, a multiple station acquisition without contrast injection was performed to obtain mask data. Immediately following the mask acquisition, a gadolinium-enhanced bolus tracking acquisition was performed with a gadolinium dose of 0.1-0.2 mmol/kg. The table translation from the first station to the second station occurred at the peak time of the contrast curve at the distal location of the second station. Table translations were 20-30 cm per step, providing 2-12 cm overlap. Hand injection and later an MR compatible power injector (Spectris MR Injector, MedRad, Pittsburgh, Pa.) was used. All infusions were followed immediately by a 30 mL saline flush.

Detailed Description Text (35):

In one patient, for example, the timing bolus arrived at the popliteal artery approximately 27 sec after injection, and it took approximately 6 sec to traverse the central station. Three-station acquisitions were planned for this subject. A 15 mL dose at 1 mL/sec injection rate was used for bolus tracking acquisition (15 sec injection time). Accordingly, table translation from the first station to the second station occurred between 34-36 sec after injection, allowing about 10 sec for imaging the first station. Imaging time at the second station was 12 sec. Then the table was translated to the third station between 48-50 sec after injection. The total acquisition time was 60 sec. All arteries from the external iliac artery in the pelvis through the anterior tibial and posterior tibial arteries at the ankle are well depicted.

Detailed Description Text (36):

Our results support the hypothesis that MRA of the lower extremity can be performed rapidly using a bolus tracking strategy, a <u>stepping</u> table, and a 2D MR <u>imaging</u> technique. With this bolus tracking MR technique, MR angiography of the entire lower extremity can be performed in approximately one minute. Including time for acquiring the scout, bolus timing and mask data <u>sets, the total</u> examination time for MRA of the entire lower extremity is between ten and fifteen minutes. This is a substantial reduction in <u>scan</u> time from that of the standard TOF technique (typically 60-90 minutes).

Detailed Description Text (37):

The 2D acquisition employed in this study provides high temporal resolution while complex subtraction of the mask image provides high contrast-to-noise ratio with minimal artifacts. A frame rate of 1-2 sec per image can be maintained while providing 1 mm.times.1 mm in-plane resolution with good SNR. This rapid acquisition enables imaging of the same contrast bolus sequentially as it transits the arterial

tree. <u>Imaging</u> of each station for five to ten seconds permits the acquisition of the contrast enhanced lower extremity arteries in 30 seconds. This is less than the time required for <u>imaging</u> one station using a 3D acquisition. Consequently, a much smaller contrast dose can be used in bolus tracking 2D MR. An alternative way to take advantage of 2D acquisition is to acquire multiple projections at each station by alternating <u>slab</u> orientation. Because the in-plane resolution is higher than that of a MIP <u>image</u> from a 3D acquisition, this may be a more effective way to obtain additional spatial information of the targeted arteries.

Detailed Description Text (38):

An alternative method to the "bolus tracking" of the preferred embodiment is to separately administer contrast agent prior to each <u>FOV</u> acquisition. In this case a mask <u>image</u> is acquired just prior to each bolus injection, the bolus is administered, and the <u>image</u> acquisition for the particular <u>FOV</u> is performed when peak contrast is obtained in that <u>FOV</u>. The table is then translated to the next <u>FOV</u> and the process is repeated.

Detailed Description Text (39):

Other data <u>processing</u> techniques may be used to generate angiograms. Methods other than complex subtraction, such as digital filters, may be used to generate angiograms. The criteria for digital filter design is to extract dynamic contrast (or signal variation) from a temporal series of <u>images</u>, and vessel contrast is determined by this dynamic contrast. For example, matched filters can be used to generate an angiogram that is a sum of individual arteriograms generated by complex subtraction.

Detailed Description Text (40):

Another application for the invention is to $\frac{\text{image}}{\text{image}}$ the aorta in the body trunk. The aortic arch and the abdominal aorta can be $\frac{\text{image}}{\text{image}}$ in two separate $\frac{\text{FOVs}}{\text{FOVs}}$ using a fast 3D acquisition technique (temporal resolution<one 3D volume per 20 sec) and contrast infusion. In addition, the table $\frac{\text{stepping}}{\text{stepping}}$ between different $\frac{\text{FOVs}}{\text{FOVs}}$ can be an important technical component for general fluoroscopic MR $\frac{\text{imaging}}{\text{imaging}}$ and $\frac{\text{MRI-guided}}{\text{interventions}}$.

CLAIMS:

- 1. A method for producing an $\underline{\text{image}}$ with an MRI system, the steps comprising:
- a) positioning a patient in the MRI system;
- b) acquiring NMR $\,\underline{image}\,$ data from the patient over a first field of view while the patient is stationary relative to the MRI system;
- c) translating the patient in the MRI system;
- d) acquiring NMR $\underline{\text{image}}$ data from the patient over a second field of view while the patient is stationary relative to the MRI system;
- e) registering the NMR \underline{image} data acquired over the first and second field of views and reconstructing an \underline{image} over a region of interest which includes the first and second field of views.
- 2. The method as recited in claim 1 in which a contrast agent is administered to the patient and the acquisition of NMR \underline{image} data over the first and second field of views occurs when the contrast agent provides substantially maximum contrast therein.
- 5. The method as recited in claim 1 in which the patient is translated additional times, NMR \underline{image} data is acquired from additional field of views, and the reconstructed \underline{image} includes NMR \underline{image} data from the additional field of views.
- 6. The method as recited in claim 1 in which the patient is translated a preselected distance and the NMR \underline{image} data acquired over the first field of view is registered with the NMR \underline{image} data acquired over the second field of view by establishing their relative positions using said preselected distance.

- 7. The method as recited in claim 1 in which the NMR image data is acquired using a local RF coil which is positioned adjacent the patient and which remains stationary as the patient is translated.
- 8. The method as recited in claim 1 in which the NMR image data is acquired using a local RF coil having a plurality of coil segments which are supported by the patient, and as the patient is translated different coil segments are switched into operation to acquire NMR image data.
- 9. The method as recited in claim 1 in which a contrast agent is administered to the patient and a timing \underline{scan} is conducted to estimate the $\underline{optimal}$ time at which \underline{step} b) is to be performed, and to estimate the velocity of the contrast agent as it flows through one of said field of view.
- 10. The method as recited in claim 9 in which the performance of $\underline{\text{step}}$ c) is determined in part by the estimated velocity of the contrast agent.
- 11. A method for producing an image with an MRI system, the steps comprising:
- a) performing a timing \underline{scan} in which a contrast agent is administered to a patient and the arrival time and the velocity of the contrast agent in a region of interest is estimated from NMR data acquired by the MRI system;
- b) performing a bolus tracking $\frac{\text{scan}}{\text{plurality}}$ to acquire NMR data from the region of interest by translating the patient to a $\frac{\text{plurality}}{\text{plurality}}$ of stations and acquiring NMR $\frac{\text{image}}{\text{image}}$ data from a corresponding $\frac{\text{plurality}}{\text{plurality}}$ of field of views within the region of interest; and
- c) reconstructing the image from NMR data acquired from all of said field of views;

wherein the start of the bolus tracking $\underline{\text{scan}}$ is determined by said estimated arrival time and the translation of the patient to said $\underline{\text{plurality}}$ of stations is timed in part by said estimated velocity.